AFOSR-TR-76-0899

1976

ADA027856

Approved for public release;
distribution unlimited.

FUNDAMENTAL RESEARCH RELATING TO NEW LASER SYSTEMS

by

Marvin L. Vestal

With Contributions By

E.M. Eyring
G. Mauclaire
J.H. Futrell

Final Report

Air Force Contract F33615-73-C-4128

March 1976

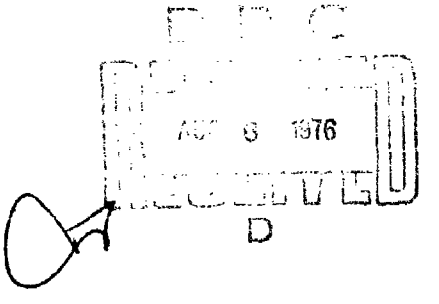

SECURITY CLASSIFICATION OF THIS PAGE (When Data Entered)

(19) REPORT DOCUMENTATION PAGE

READ INSTRUCTIONS BEFORE COMPLETING FORM

(18) REPORT NUMBER: AFOSR TR-76-0899

2. GOVT ACCESSION NO.

3. RECIPIENT'S CATALOG NUMBER

4. TITLE (and Subtitle)

(6) FUNDAMENTAL RESEARCH RELATING TO NEW LASER SYSTEMS,

5. TYPE OF REPORT & PERIOD COVERED

(9) Final report,

6. PERFORMING ORG. REPORT NUMBER

7. AUTHOR(s)

(10) Marvin L. Vestal

8. CONTRACT OR GRANT NUMBER(s)

(15) F33615-73-C-4128

9. PERFORMING ORGANIZATION NAME AND ADDRESS

Department of Chemistry
University of Utah
Salt Lake City, Utah 84112

10. PROGRAM ELEMENT, PROJECT, TASK AREA & WORK UNIT NUMBERS

(16) AF - 9538-01, 61102F, 681303

(17) 9538-01

11. CONTROLLING OFFICE NAME AND ADDRESS

AF Office of Scientific Research/NC
Bolling AFB, Building 410
Washington, D.C. 20332

12. REPORT DATE

(11) Mar[redacted]76

13. NUMBER OF PAGES

80

14. MONITORING AGENCY NAME & ADDRESS (if different from Controlling Office)

(12) 81p.

15. SECURITY CLASS. (of this report)

Unclassified

15a. DECLASSIFICATION/DOWNGRADING SCHEDULE

16. DISTRIBUTION STATEMENT (of this Report)

Approved for public release; distribution unlimited.

17. DISTRIBUTION STATEMENT (of the abstract entered in Block 20, if different from Report)

18. SUPPLEMENTARY NOTES

19. KEY WORDS (Continue on reverse side if necessary and identify by block number)

20. ABSTRACT (Continue on reverse side if necessary and identify by block number)

A new tandem Quadrupole mass spectrometer, developed explicitly for photo-dissociation experiments on both positive and negative ions, is described. This unique instrument employs crossed-beam techniques to achieve high sensitivity and precise specification of the observed photodissociation of photodissociation cross sections as a function of wavelength for ions of aeronomic importance or of potential importance in the development of new laser systems. Results are given for CO3 minus, CO4 minus, CO4 minus, O2 plus, O3 plus, O4 plus, O2 minus, O3 minus, Ne2 plus, Ar2 plus, and (CO2)2 plus.

DD FORM 1 JAN 73 1473 EDITION OF 1 NOV 65 IS OBSOLETE 4/00 730 UNCLASSIFIED

SECURITY CLASSIFICATION OF THIS PAGE (When Data Entered)

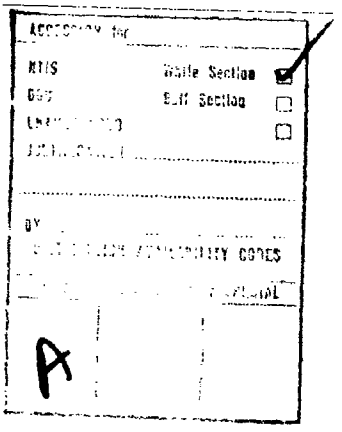

Abstract

A new tandem Quadrupole mass spectrometer, developed explicitly for photodissociation experiments on both positive and negative ions, is described. This unique instrument employs crossed-beam techniques to achieve high sensitivity and precise specification of the observed photodissociation reactions. The research effort was concerned primarily with measurements of photodissociation cross sections as a function of wavelength for ions of aeronomic importance or of potential importance in the development of new laser systems. Results are given for CO_3^-, CO_4^-, O_2^+, O_3^+, O_4^+, O_2^-, O_3^-, Ne_2^+, Ar_2^+, and $(CO_2)_2^+$.

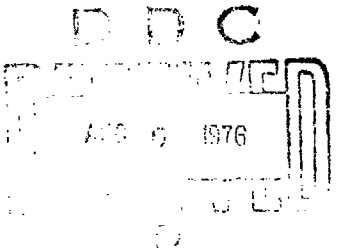

TABLE OF CONTENTS

List of Figures

List of Tables

PHOTODISSOCIATION EXPERIMENTS

I. INTRODUCTION

In this research a new tandem quadrupole photodissociation mass spectrometer has been developed and applied to fundamental studies on the photochemistry of positive and negative ions of atmospheric importance. This unique instrument employs crossed-beam techniques to achieve high sensitivity and precise specification of the observed reaction. The photon-ion collision occurs in high vacuum (10^{-8} torr) effectively removing the possibility that the results might be affected by concurrent collisional processes. The ionization source which was developed explicitly for this work allows the production of intense beams of both positive and negative ions. These range from the parent and fragment ions produced by electron impact under low pressure conditions to the energetically relaxed products of ion-molecule reactions obtained under high pressure conditions, including both positive and negative cluster ions. The instrument has been operated both with a 200 watt Hg lamp and high-intensity monochrometer, and with a tunable dye laser. Using the laser as the light source greatly extends the capabilities of the instrument, and with the laser, high resolution (3 cm^{-1}) photodissociation spectra have been obtained without sacrificing sensitivity.

In this research we have concentrated primarily on ions of aeronomic importance.[1] Photodissociation cross sections have been measured as a function of wavelength for CO_3^-, CO_4^-, O_2^+, O_3^+, O_4^+, O_2^-, and O_3^-. The effect of ion-source pressure on the observed photodissociation cross sections has been studied for several of these ions and data has been obtained on the collisional relaxation of long-lived excited states of CO_3^- and O_2^+. Preliminary investigations were conducted on several other ions of aeronomic interest, including O_4^-, NO_2^-, NO_3^-, $H_3O^+.H_2O$, $OH^-.H_2O$, and $H_3O^+.2H_2O$, but

photodissociation was not observed. Results were obtained on the photodissociation of Ne_2^+, Ar_2^+, and $(CO_2)_2^+$ of dimer ions. The $(CO_2)_2^+$ ion is particularly interesting since the measured photodissociation cross section is the largest observed in this work (2×10^{-17} cm^2) and the maximum cross section occurs at the red end of the visible spectrum. These results may have important implications with respect to the ionospheric chemistries of Mars and Venus.[2]

II. BACKGROUND

The dissociation of ions by photon impact, apart from intrinsic interest as a basic photochemical process, is potentially a very important new area of research for the following reasons: (1) Approximate theoretical calculations can be made of photodissociation cross-sections in simple systems, and it is essential to develop experimental data for comparison with theoretical predictions. (2) If a well-defined threshold is observed, the energy of the photodissociation threshold will provide bond dissociation energies of precision far greater than presently available for ionized systems. (3) A stringent test of unimolecular dissociation is provided by the possibility of depositing a precisely known quantum of energy in an ion whose internal energy states are well specified. (4) High-resolution photodissociation experiments will permit the assignment of vibrational structure leading to a knowledge of symmetry and bonding in simple ions. (5) Determination of even broad features of wavelength dependence of the dissociation process will give interesting information on upper electronic energy levels of ionic species. (6) Information can be obtained in much greater detail than is now available on the population of excited states in ion beams prepared in various ways and on the lifetimes of various excited states.

In view of the potential utility of photodissociation studies for characterizing energy states of ions, the almost total absence of experimental data must be attributed to the lack of sensitive and convenient means for observing them. This results from the fact that cross-sections for these processes are rather small, and from the fact that all experiments attempted to date have the intrinsic difficulty of isolating the photodissociation even from all other chemical processes which are occurring simultaneously. Several calculations and measurements have been made of the cross-section and wave length dependence of the H_2^+ photodissociation[3,4] and this process has a cross-section in the neighborhood of $10^{-18}cm^2$ with well-resolved vibrational structure. Dunn[3] has observed photodissociation of N_2^+ near the limits of sensitivity of his apparatus and estimates a cross-section value of 1×10^{-17} cm^2. He has also obtained an upper limit of 10^{-20} cm^2 for the photodissociation cross-section of H_3^+.

Busch and Wilson[5] used a molecular beam and a ruby laser to study NO_2 and NOCl neutrals. They determined the symmetries of the dissociating states, the lifetimes of these states, the energy partition of the dissociation, and observed the presence of vibrational excitation in the molecular fragment. Diesen, Wahr, and Adler[6] used a similar experiment to determine the bond energy of Cl_2. Ozenne, Pham, and Durup[7] obtained kinetic energy spectra of H^+ ions produced by photodissociation of 4 keV H_2^+ ions by a ruby laser polarized either parallel or perpendicular to the ion beam. Structure reflecting the vibrational levels of the primary ions was observed. Los and Maas[8] have also investigated H_2^+ using 10 keV ions and an Ar^+ laser.

The technique of ion cyclotron resonance has been applied by Dunbar[9] and has provided the first quantitative information on photodissociation of the ions CH_3Cl^+, N_2O^+ and certain hydrocarbon ions.[10] The ICR spectrometer, operated in the trapped ion mode can hold ions in the photon beam for periods

of the order of seconds. This permits photodissociation processes to be observed with wavelength-selected light. The photodissociation cross-section for N_2O^+ was estimated to be 0.2×10^{-18} cm^2 without strong wavelength dependence between 4,000 and 6,500 Angstroms. Photodissociation studies of CH_3CO^+ showed a broad peak at 3150 Angstroms having a cross-section of 8×10^{-18} cm^2. This provided the first quantitative data on gas phase photodissocation processes for molecules of low symmetry.

These ion cyclotron resonance experiments are most interesting in that they provide us the first quantitative data on these processes using a technique which can be generalized to other systems. They suffer the drawback that the total ion beam is illuminated and one must, of necessity, search for small signal changes in large numbers and discriminate among several dissociation processes in order to determine which cation leads to a particular dissocation product. Therefore, it is unlikely that the ion cyclotron resonance method will actually realize the generality of which it appears to be capable.

The long storage time of the ICR experiment produces extremely stringent requirements of vacuum if ion neutral collision processes during the excitation and observation time are not to be a complicating factor. For a typical ion neutral collision rate coefficient of the order of 10^{-9} cm^3/molecule-sec., an ion storage time of one second, and the requirement that only one tenth of the ions experience a collision requires that the neutral molecule pressure be equal to or less than 10^8 molecules/cm^3. This corresponds to a pressure of 3×10^{-9} torr in the ICR cell. The primary ion current for an electron current of 10^{-5}amp., ionization path length of 2 cm and 2.5×10^{-16} cm^2 ionization cross-section at this pressure is only $5 \times 10^{-}13$ amp. This is near the detection limit of ion cyclotron resonance experiments, and the experiments referred to above have been carried out at substantially higher pressures where ion-neutral collisions are

certainly a complicating factor. There does not appear to be any way to enhance significantly the detection sensitivity of ion cyclotron resonance experiments, and the technique will be of limited utility in characterizing elementary ion-photon excitation processes.

Moseley, Cosby, Bennet, and Peterson[11,12] have adapted a drift tube mass spectrometer for photodissociation studies on negative ions. This instrument employs an ion source and drift region filled with a gas or gas mixture at a pressure in the range 0.05 to 1.0 torr. Ions are formed by electrons which are extracted with controlled energy from a thoria-iridium filament. After entering the drift region, the ions drift under the influence of a weak uniform electric field toward the extraction aperture. During this drift, the ion swarm spreads due to diffusion, and new ion species may be formed through ion-molecule reactions with the drift gas. Just before exiting the drift region, the ions can be intersected by photons of a selected energy. After passing through the 0.1 cm diameter extraction aperture, the ions enter a high vacuum chamber and are accelerated to about 40 eV and focused into a quadrupole mass spectrometer. Ions of the selected mass to charge ration are detected by an electron multiplier and counted individually.

Two different laser configurations have been used as photon sources with this instrument. Photon energies between 2.34 and 2.71 eV were obtained by seven discrete lines of a commercial 4 watt argon ion laser. The laser was operating in the TEM_{00} transverse mode with the drift tube intracavity. In this configuration it provided circulating powers ranging from 5 watts to 100 watts for the various lines with a beam diameter of approximately 0.15 cm. Photon energies between 1.93 and 2.19 eV were obtained using a commercial "jet-stream" dye laser pumped by the multiline output beam of the argon ion laser. In this configuration the drift tube was contained in the cavity of the

dye laser. Using an ethylene glycol solution of Rhodamine 6G dye, the laser was continuously tunable from 640 to 565 nm. It provided circulating powers of 3 to 40 watts over this range with a bandwidth of less than 0.05 nm and a beam diameter of 0.2 cm.

This instrument has been applied to studies on photodissociation and photodetachment of a number of ions of importance to the chemistry of the upper atmosphere including O_2^-, O_3^-, O_4^-, CO_3^-, HCO_3^-, and $CO_3^-.H_2O$. The drift tube instrument appears to provide an extremely powerful technique for measuring total photodestruction cross sections for negative ions. However, the fact that the interaction between the light beam and the ions occurs in a high pressure region where a number of ions other than the selected reactant are usually present (often including the photodissociation product ion) seriously complicates the problem of discriminating between photodetachment and photodissociation.

III. EXPERIMENTAL APPARATUS AND TECHNQIUES

A. The Tandem Quadrupole Photodissociation Mass Spectrometer

This instrument was designed and constructed during the present work specifically for photodissociation studies. The apparatus is shown schematically in Figure 1, and a block diagram of the system is shown in Figure 2. The instrument consists of an ion source region which is fitted with a dual mode electron impact/chemical ionization ion source and gas inlets, a quadrupole primary mass/charge analyzer, a reaction region with quadrupole ion trapping, a quadrupole secondary mass/charge analyzer, electron multiplier ion detector, and the necessary electronics. A beam of modulated, wavelength-selected light intersects the ion beam near the center of the reactor quadrupole.

As shown in Figure 1, three stages of differential pumping are employed.

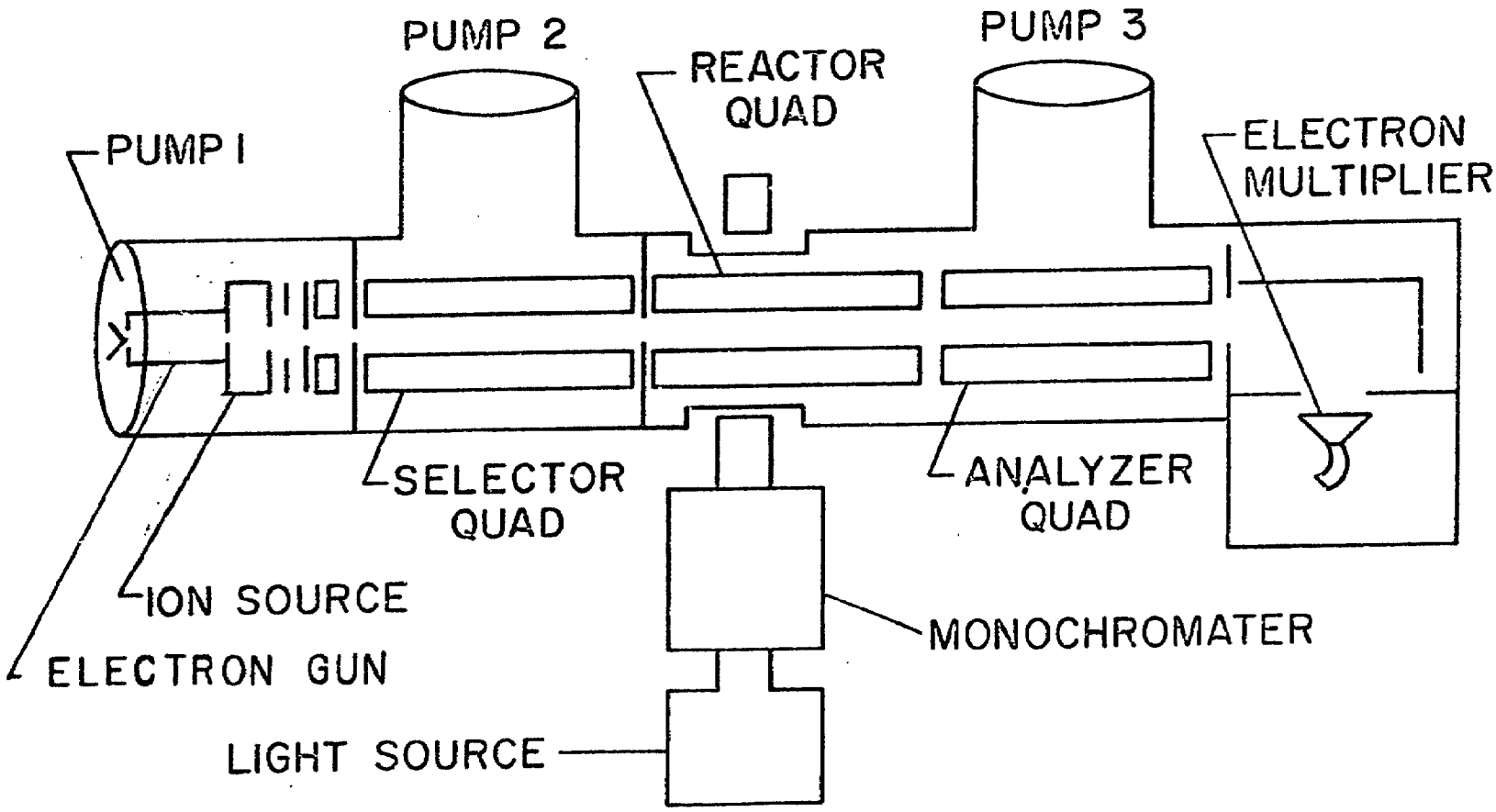

Fig. 1. Schematic diagram of the tandem quadrupole photodissocation mass spectrometer.

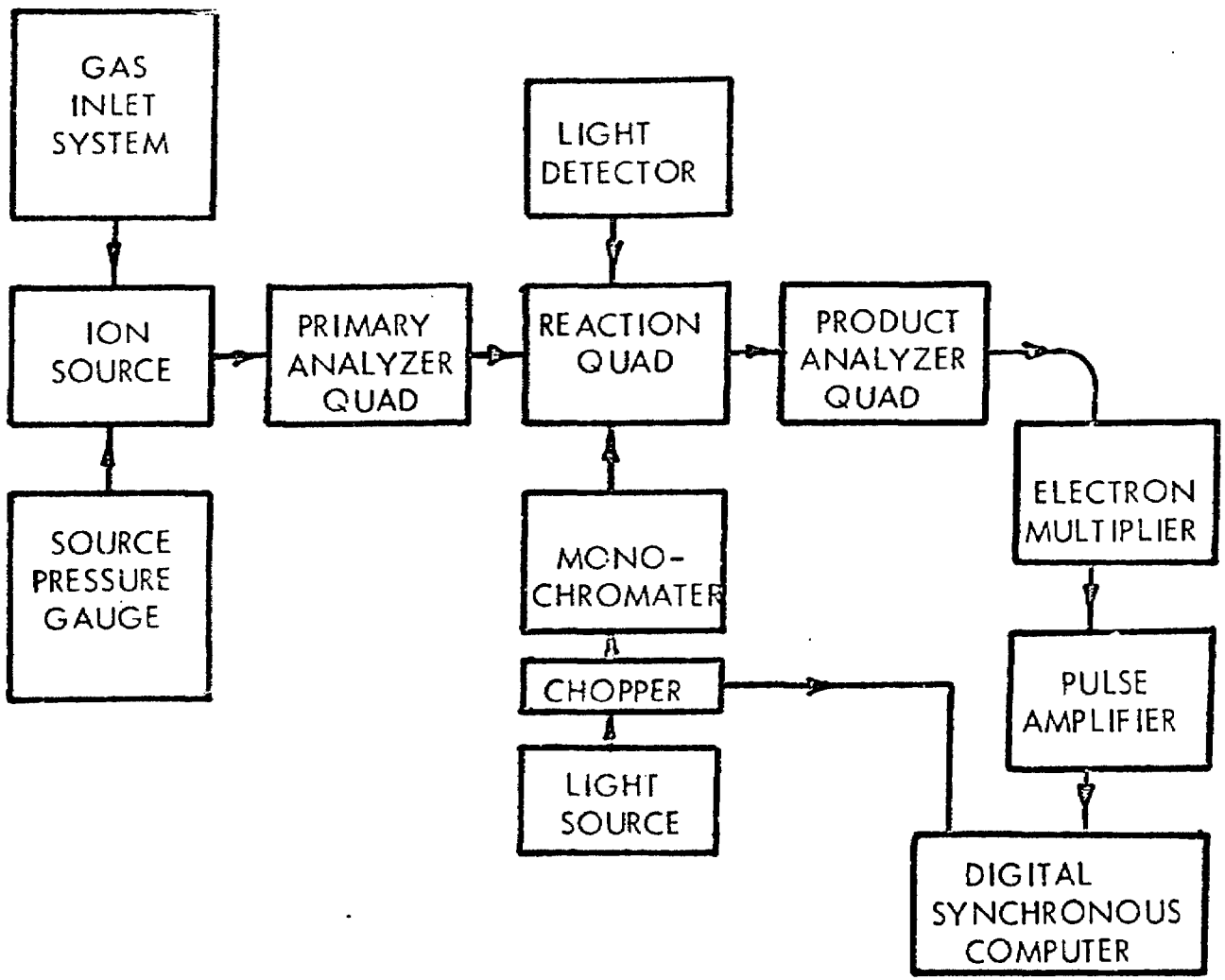

Figure 2. Block diagram of the tandem quadrupole photodissociation mass spectrometer.

The ion source region is evacuated by a 1200 liter/sec diffusion pump[13] with minimum baffling to maximize throughput. The selector quadrupole region and the reactor and analyzer quadrupole region are separatedly pumped by 1200 liter/sec diffusion pumps equipped with liquid nitrogen baffles.[14] Background pressures in the reactor and analyzer quadrupole regions is typically 2×10^{-8} torr with ca. 1 torr in the high pressure ion source.

Ions are produced in a dual mode electron impact/chemical ionization source which was developed explicitly for this work. This source can produce intense beams of a wide variety of both positive and negative ions. These species range from the parent and fragment ions produced by electron impact under low pressure conditions to the energetically relaxed products of ion-molecule reactions obtained under high pressure conditions, including both positive and negative cluster ions. Mass resolved ion beams in excess of 10^{-9} amperes are usually obtained for the more intense peaks in a given spectrum.

The light source used in the first series of experiments is a 200 watt super pressure Hg lamp.[15] Wavelength selection is accomplished using a small, high efficiency grating monochromater.[15] Quartz lenses provide the necessary focusing and the light beam pass into and out the vacuum chamber through optical grade sapphire windows. The light from the monochromater is focused into the space between the rods of the reactor quadrupole, passes on through and is detected by a thermistor radiometer.[16] The light spectrum measured with this arrangement is shown in Figure 3, where the monochromater resolution is 22 nm.

The light is chopped mechanically by a rotating segmented disc. The state of the light beam is sensed by an auxilliary light beam and photodiode detector located so that the auxilliary beam is chopped synchronously with the main light beam. The signal from the photodiode is used to gate the digital synchronous computer between the signal and background channels.

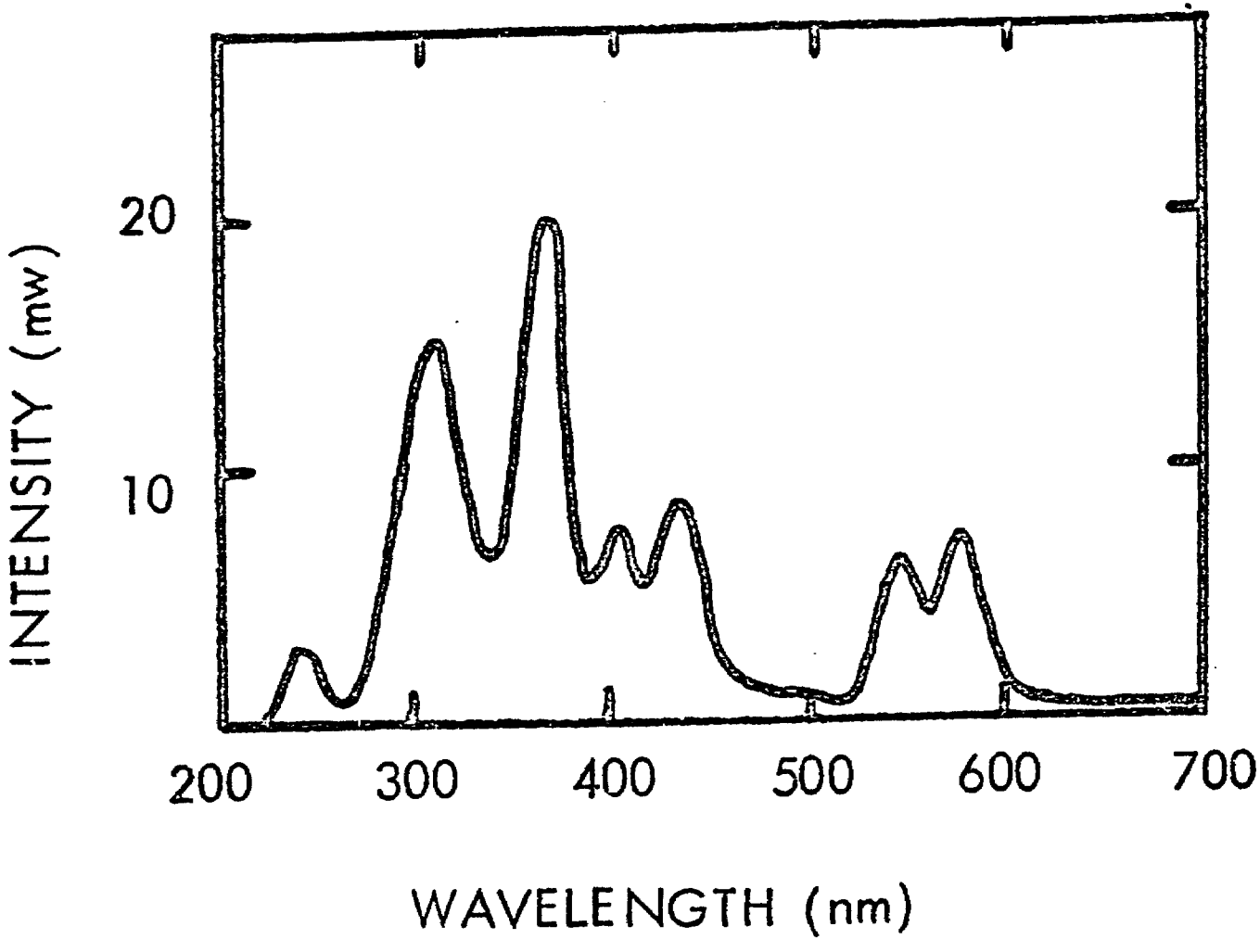

Figure 3. Spectrum of the 200 watt super pressure Hg lamp measured at a resolution of 22 nm. Intensities were measured using the thermistor radiometer.

The photodissociation mass spectrometer has also been operated with a commercial dye laser pumped by a xenon flash lamp.[17] With proper selection of dyes this laser provides continuously tunable radiation throughout the visible spectrum with a resolution of 3 cm^{-1}. It is also equipped with a frequency doubling accessory which allows operation in the UV. The output consists of light pulses approximately 1 μ sec in duration at repitition rates selectable from 5 to 30 pulses per second. The light beam diameter is approximately 2 mm at the half-integral points and angular divergence is less than 1 milliradian. Approximate output powers and tuning ranges for the various dyes are summarized in Table I.[18]

The tunable dye laser greatly extends the capabilities of the tandem quadrupole photodissociation mass spectrometer. The band width is about two orders of magnitude narrower than that for which useable intensity can be obtained using the mercury lamp and monochromater while the average output power is about one order of magnitude larger for the laser. Furthermore, the fact that the light output is concentrated in pulses of short duration leads to a substantial improvement in signal-to-noise ratio, since product ions are only counted during the short time interval following the light pulse during which photodissociation products may reach the detector.

B. Experimental Techniques

The primary ions to be studied are selected according to their mass/charge by the primary or selector quadrupole and transmitted to the reactor quadrupole where the ion beam and the photon beam intersect. If a photon absorption occurs and results either in fragmentation or further ionization, a product ion of a different mass/charge ratio is produced. The secondary analyzer quadrupole is tuned to pass only the particular product ion under study. The

Table I. DYE RANGES AND POWER CURVES

Curve	Dye	Tuning Range (nm)	Peak Gain Wavelength (nm)	Wavelength Scale
1	Coumarin 120	435-455	442	A
2	Coumarin 2	445-482	460	A
3	Coumarin 102	476-518	490	B
4	Coumarin 30	493-540	512	B/C
5	Coumarin 6	521-558	540	C
6	Sodium Fluorescein	542-577	558	C/D
7	Rhodamine 575 (1:1 water/ Methanol)	566-610	590	D
8	Rhodamine 6G (1:1 water/ Methanol)	577-625	598	D
9	Rhodamine 6G (4% Ammonyx LO)	585-633	610	D
10	Kitton Red S	622-665	642	D/E
11	Cresyl Violet	655-700	673	E
12	Oxazine 170	675-730	705	E/F

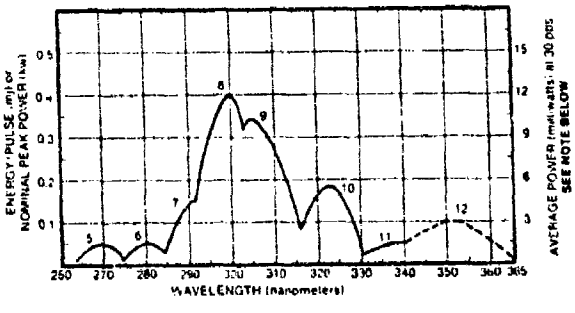

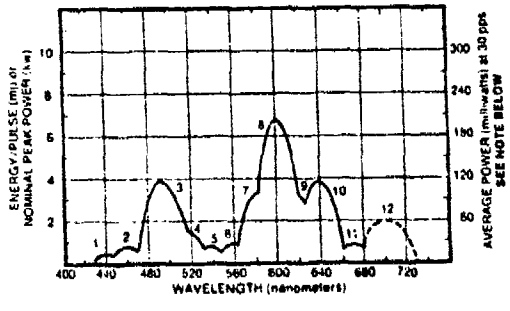

NOTE: Dashed curves are for peak powers and energy per pulse only, not average power.

transmitted ions are detected by an electron multiplier; the pulses are amplified and counted using an SSR Model 1110 Digital Synchronous Computer.[19] This instrument contains a two channel scaler which is gated by a signal from the light beam chopper. Ions received in phase with the "on" time of the light beam are accumulated in the signal channel and ion pulses received in phase with the "off" time of the light source are accumulated in background channel. These counts may be accumulated for a preset number of chopper cycles and the signal, background, sum, and difference counts can be selectively displayed on a front panel digital meter.

The intensity of the photodissociation product ion signal is given by

$$I_2 = (D \pm \sqrt{S})/N\tau \qquad (1)$$

where D is the difference count (signal channel - background channel), S is the total count (signal channel + background channel) accumulated during N cycles, where τ is the chopper period or the time between laser pulses.

The photodissociation cross section is given by

$$\sigma = \frac{I_2}{n_1 F_\lambda \Delta V} \qquad (2)$$

where ΔV is the interaction volume, n_1 is the average reactant ion density (number/cm^3) in ΔV, F_λ is the average photon flux (photons/cm^2-sec) through ΔV, and I_2 is the product intensity (ions/sec). Assuming that the ion density is uniform in ΔV, and that the entire ion beam intersects the light beam, then

$$n_1 = I_1 / A_1 v_1 \qquad (3)$$

where A_1 is the cross sectional area of the ion beam, v_1 is the average velocity, I_1 is the primary ion beam intensity (ions/sec), and

$$\Delta V = A_1 \cdot \Delta x \qquad (4)$$

where Δx is the width of the light beam at the half-integral points. Making these substitutions gives

$$\sigma = \frac{I_2}{I_1 F_\lambda \tau} \tag{5}$$

where $\tau = \Delta x/v_1$ is the average time that an ion spends in the photon beam. In applying equation (5) to the determination of absolute cross sections the major uncertainty is in τ. The average ion velocity is computed from the difference in potential between the ion source and the centerline of the reactor quadrupole. Experiments in which the ion transmission is measured as a function of this potential difference indicate that the ion energy distribution is about 0.5 eV in width (full width at half-maximum). In varying the ion energy over the range from 1 to 10 eV the cross sections computed accordingly to equation (5) are observed to be constant to within $\pm$ 10%, indicating that the average ion energy as determined in this way is a satisfactory measure of the ion velocity. The half-integral width of the light beam, Δx was determined by stopping down the light beam until the total intensity was reduced by one-half. These measurements gave Δx = 0.2 cm for the laser beam and 0.5 cm for the beam from the monochromater. The height of the light beam is limited to 0.3 cm by the spacing between the quadrupole rods, and the diameter of the ion beam entering the reactor quadrupole is defined by an 0.3 cm aperture between the primary ion selector quadrupole and the reactor quadrupole. The measured transmission of primary ions through the reactor quadrupole is greater than 99% indicating that the quadrupole, acting as a strong-focusing lens, is effective in maintaining the collimation of the ion beam. Thus we estimate that at least 80-90% of the ions pass through the photon beam. Overall, the estimated uncertainty in τ is less than $\pm$ 20%.

The light flux is monitored with a thermistor radiometer which is

calibrated by the manufacturer to a stated accuracy of 2%.[16] With the Hg lamp the measured flux during a run was typically constant to within about 5%. With the laser light source some short term fluctuations were occasionally encountered, although there were generally less than 10% of the average intensity. Any runs in which larger fluctuations were observed were discarded.

The intensity of the primary ion beam, I_1, was measured by setting the secondary ion analyzer to transmit the primary ion beam and measuring the current to the Faraday cup with an electrometer. This measurement was routinely done at the beginning and end of each measurement of product intensity, and the observed drift was generally less than 10 per cent. If the observed drift exceeded 10 per cent the run was discarded.

The counting efficiency for detection of product ions by the electron multiplier was determined by setting both the primary and secondary quadrupole analyzers to transmit product ions produced in the ion source. The ion source was then adjusted until the beam intensity was on the order of 10^{-13} amp. The ions were counted with the same multiplier voltage settings used in detecting photodissociation product ions. The counting rates observed were typically within 10 per cent of those calculated from the Faraday cup measurements, indicating a counting efficiency of at least 90 per cent.

All of the systems studied have involved relatively large mass differences between product and reactant, thus allowing the product ion analyzer quadrupole to be operated at low resolution where mass discrimination is minimal. While serious mass discrimination has been observed at higher resolutions, measurements of ion transmissions through the product analyzer quadrupole under the conditions used for most of this work indicate that the discrimination is less than 5 per cent.

Overall the estimated error limits on the reported absolute cross sections

are ± 30 per cent. The relative errors due to counting statistics and short term fluctuations in light intensity are generally substantially smaller and are shown as error bars on the data. If the product ions were ejected primarily in the direction perpendicular to the axis of the quadrupoles with substantial kinetic energies, it is possible that some additional discrimination could occur which has not been taken into account. Since the laser beam is polarized parellel to the axis of the quadrupoles, this could only occur if the transition dipole were orthogonal to the dissociating bond. The fact that the observed cross sections are found to be independent of ion velocity through the interaction region suggests that this is not an important source of error in any of the present work.

C. Sensitivity

The major source of noise in the tandem quadrupole photodissociation mass spectrometer is due to collision induced dissociation. This noise is the principal factor limiting sensitivity of the instrument. The intensity of the photodissociation signal is given by

$$I_2 = I_1 F_\lambda \tau \sigma \qquad (6)$$

where I_1 is the reactant ion current (amperes or number/sec), τ is the time a reactant ion interacts with the photon beam (sec), F_λ is the average photon flux (number/cm^2sec), and σ is the photodissociation cross section (cm^2).

In the chopped DC mode of operation the noise due to collision induced dissociation is given by

$$N = fI_1 \qquad (7)$$

where the factor f varies between 10^{-4} and 10^{-6} for a variety of ions that have been studied in our work to date. The signal to noise ratio is

$$I_2/N = \sigma F_\lambda \tau / f \tag{8}$$

One of the cases we have studied (methyl bromide) corresponded to the following values of these parameters; $f = 10^{-6}$, $F_\lambda = 4 \times 10^{16}$ photons/cm^2sec, $\tau = 10^{-5}$ sec, which gives signal/noise = $4 \times 10^{17}\,\sigma$. Thus at the larger cross sections ($5 \times 10^{-18} cm^2$) the signal to noise ratio is about 2 and at the smaller cross sections for which we have been able to obtain data ($2 \times 10^{-20} cm^2$) the signal is less than 1 per cent of noise. The statistical standard deviation of a measurement of I_2 is given by

$$S.D. = \sqrt{(I_2 + 2N)t} \tag{9}$$

where I_2 and N are the average signal and noise given by equations (6) and (7), respectively, and t is the counting time.

The pulsed light source from the laser greatly improves the sensitivity by reducing the effective noise. For the same average photon flux the average signal is the same as for the chopped mode, but the noise is given by

$$N = Rt_1 f I_1 \tag{10}$$

where R is the pulse repetition rate, and t_1 is the time interval per pulse that ion counts are accepted by the gated electronics. For the pulsed system with R = 30/sec and $t_1 = 3 \times 10^{-6}$sec., the noise is effectively reduced by a factor of 10^4 over that obtained with the chopped DC light source. Data on sensitivity is summarized in Figure 4, where the relative standard deviation for I_2 is plotted as a function of counting time for several operating conditions. As can be seen from Figure 4, the minimum photodissociation cross section that can be detected under the "most favorable" conditions in a reasonable maximum counting time of 8 hours is about $10^{-24} cm^2$, while under the "least" favorable conditions cross sections of $3 \times 10^{-22} cm^2$ can be detected.

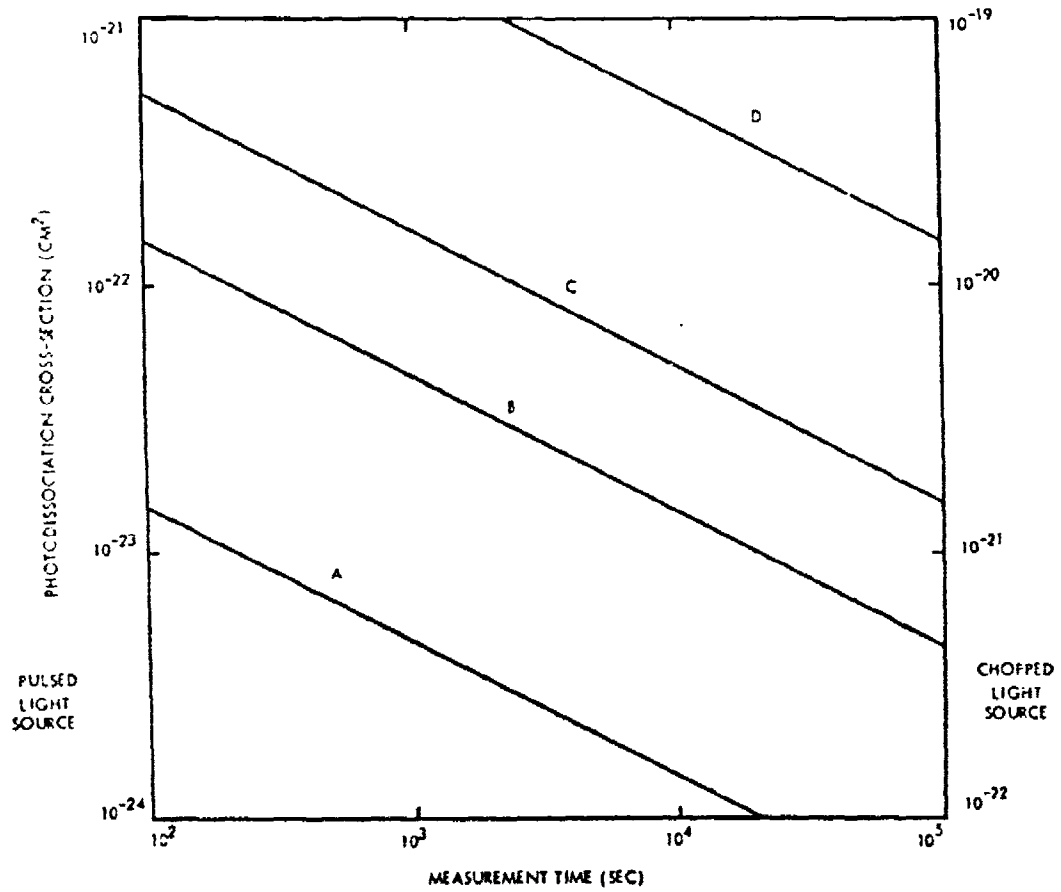

Figure 4. Calculated measurement time required to give signal standard deviation equal to average signal as a function of photodissociation cross section for several operating conditions (A) -"most favorable" case $I_1 = 1 \times 10^{-8}$ amps, $f = 10^{-6}$, (B) $I_1 = 1 \times 10^{-8}$ amps, $f = 10^{-4}$, (C) $I_1 = 1 \times 10^{-11}$, $f = 10^{-6}$, similar to conditions used in measuring dissociation of CH_3Br^+ (D) "least favorable" case, $I_1 = 1 \times 10^{-11}$ amps, $f = 10^{-4}$, I_1 is the reactant ion current, and f is the fraction of I_1 which is collisionally dissociated.

IV. RESULTS AND DISCUSSION

A. Introduction

The results are presented approximately in the chronological order in which the studies on each system were begun. The first reaction studied was

$$CH_3Cl^+ \xrightarrow{h\nu} CH_3^+ + Cl \qquad (R1)$$

which had been studied previously by Dunbar using the ICR trapped-ion technique. We also studied the analogous reaction for methyl bromide. (R2) These initial studies were undertaken primarily for the purpose of evaluating the apparatus and establishing the experimental techniques. The reaction

$$SF_6^- \xrightarrow{h\nu} SF_5^- + F \qquad (R3)$$

was investigated in conjunction with establishing the techniques for studying negative ions.

The major emphasis in this work was placed on ionic systems of importance in ionospheric chemistry. Results were obtained for the following reactions

$$CO_3^- \xrightarrow{h\nu} O^- + CO_2 \qquad (R4)$$

$$CO_4^- \xrightarrow{h\nu} O_2^- + CO_2 \qquad (R5)$$

$$CO_4^- \xrightarrow{h\nu} CO_3^- + O \qquad (R6)$$

$$O_2^+ \xrightarrow{h\nu} O^+ + O \qquad (R7)$$

$$O_3^+ \xrightarrow{h\nu} O^+ + O_2 \qquad (R8)$$

$$O_3^+ \xrightarrow{h\nu} O_2^+ + O \qquad (R9)$$

$$O_4^+ \xrightarrow{h\nu} O_2^+ + O_2 \qquad (R10)$$

$$O_2^- \xrightarrow{h\nu} O^- + O \qquad \text{(R11)}$$

$$O_3^- \xrightarrow{h\nu} O^- + O_2 \qquad \text{(R12)}$$

$$O_3^- \xrightarrow{h\nu} O_2^- + O \qquad \text{(R13)}$$

Preliminary investigations were conducted on several other ions of aeronomic interest, but photodissociation was not observed. Systems studied for which no positive results were obtained include O_4^-, NO_2^-, NO_3^-, $H_3O^+.H_2O$, and $H_3O^+.2H_2O$. Some indication of photodissociation of O_4^- was seen with a cross section on the order of 10^{-18} cm^2 but the combination of the rather small maximum intensities of O_4^- (5×10^{-13} amp) produced within the range of operating conditions of the ion source, and the rather high collision-induced background, precluded our making quantitative measurements. Photodissociation cross sections for NO_2^- and NO_3^- appear to be less than 10^{-20} cm^2 throughout the entire visible and UV portion of the spectrum accessible in these studies. This is consistent with available energetic data for these ions.[20] The water cluster systems all show a very large collision-induced component which prevented very sensitive measurements on these systems, but the photodissociation cross sections do not appear to be significantly larger than 10^{-18} cm^2.

Results were obtained for the following ion cluster dissociations

$$Ne_2^+ \xrightarrow{h\nu} Ne^+ + Ne \qquad \text{(R14)}$$

$$Ar_2^+ \xrightarrow{h\nu} Ar^+ + Ar \qquad \text{(R15)}$$

$$(CO_2)_2^+ \xrightarrow{h\nu} CO_2^+ + CO_2 \qquad \text{(R16)}$$

These reactions all apear to involve direct transitions from a bound initial state to a repulsive final state. The cross section measured for

the photodissociation of the $(CO_2)_2^+$ dimer (2×10^{-17} cm^2) at the red end of the visible spectrum were the largest observed for any reaction studied in this work. These results may have important implications with respect to the ionospheric chemistries of Mars and Venus.[2]

B. Methyl Chloride and Methyl Bromide

The results obtained on these two systems, using the Hg light source, have been published [21] and will only be reviewed briefly here. Results obtained for the reaction

$$CH_3Cl^+ \xrightarrow{h\nu} CH_3^+ + Cl \qquad (R1)$$

are given in Figure 5. The region to the long-wavelength side of the thermochemical threshold for reaction from ground state CH_3Cl^+ has also been studied using the laser. In the 590 nm to 620 nm region no photodissociation was observed giving as upper limit on the cross section of 5×10^{-21} cm^2. Thus it appears that there is no significant amount of vibrational excitation of the CH_3CL^+.

Our published results for the reaction

$$CH_3Br^+ \xrightarrow{h\nu} CH_3^+ + Br \qquad (R2)$$

are given in Figure 6. In addition we have investigated the region from 590 to 622 nm using the tunable dye laser. These results, which are given in Figure 7, illustrate the high sensitivity obtainable using the laser. The statistical precision of these results range from about $\pm$ 1% near the band maximum (605 nm) to about $\pm$ 5% at the extremes even thought the photodissociation cross sections are rather small in this region (ca. 10^{-20} cm^2).

C. Sulfur Hexafluoride

Results obtained on the reaction

$$SF_6^- \xrightarrow{h\nu} SF_5^- + F \qquad (R3)$$

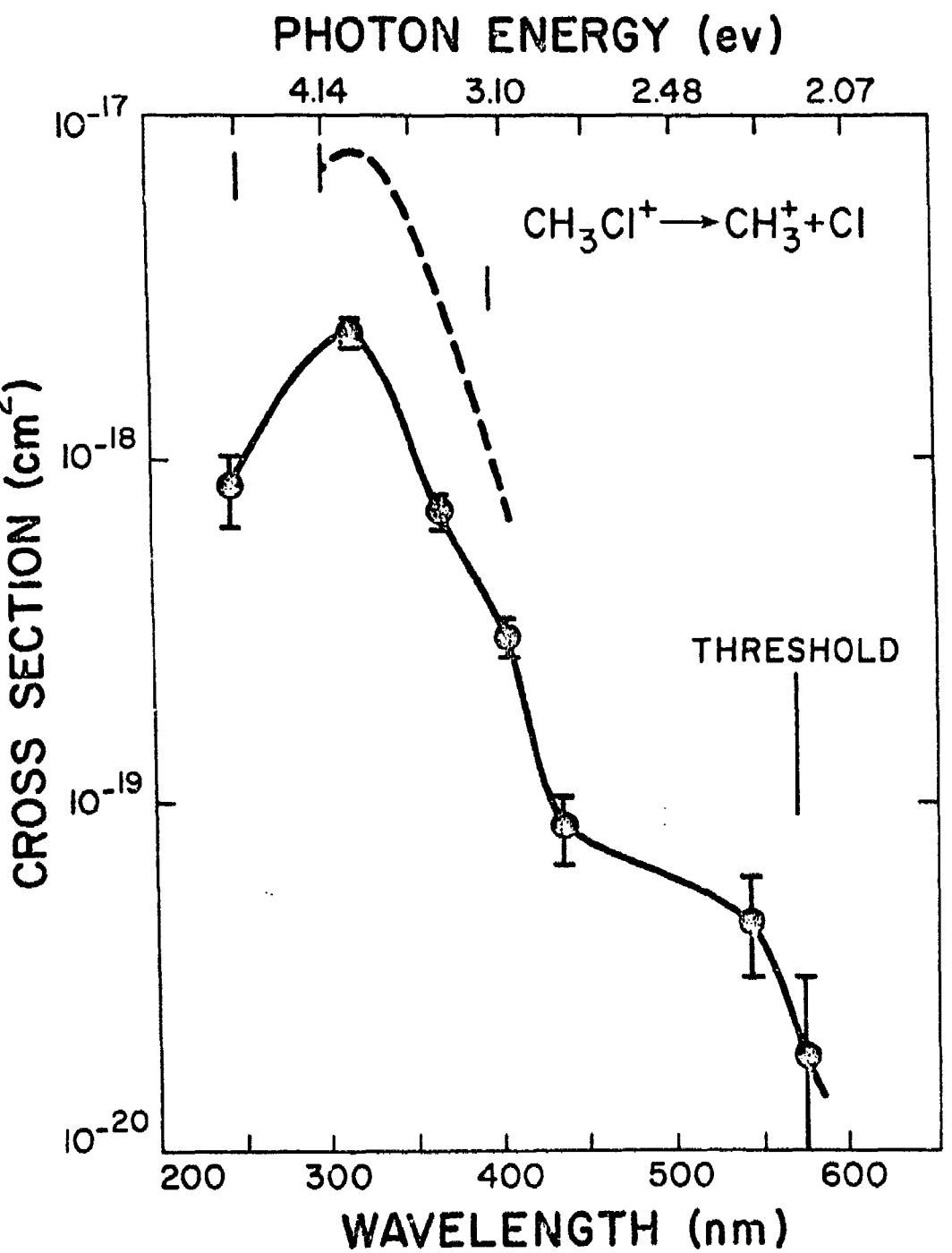

Fig. 5.

Experimental results for the photodissociation of CH_3Cl^+. The treshold for dissociaiton is calculated from heats of formation and assumes the primary ion is formed initially in its ground electronic and vibrational state. The vertialy lines indicate the expected locations of peaks corresponding to photo-induced transitions from the ground state of the ion to the electronically excited states determined from photoelectron spectroscopy. The dashed line is the result of Dunbar, ref. (9).

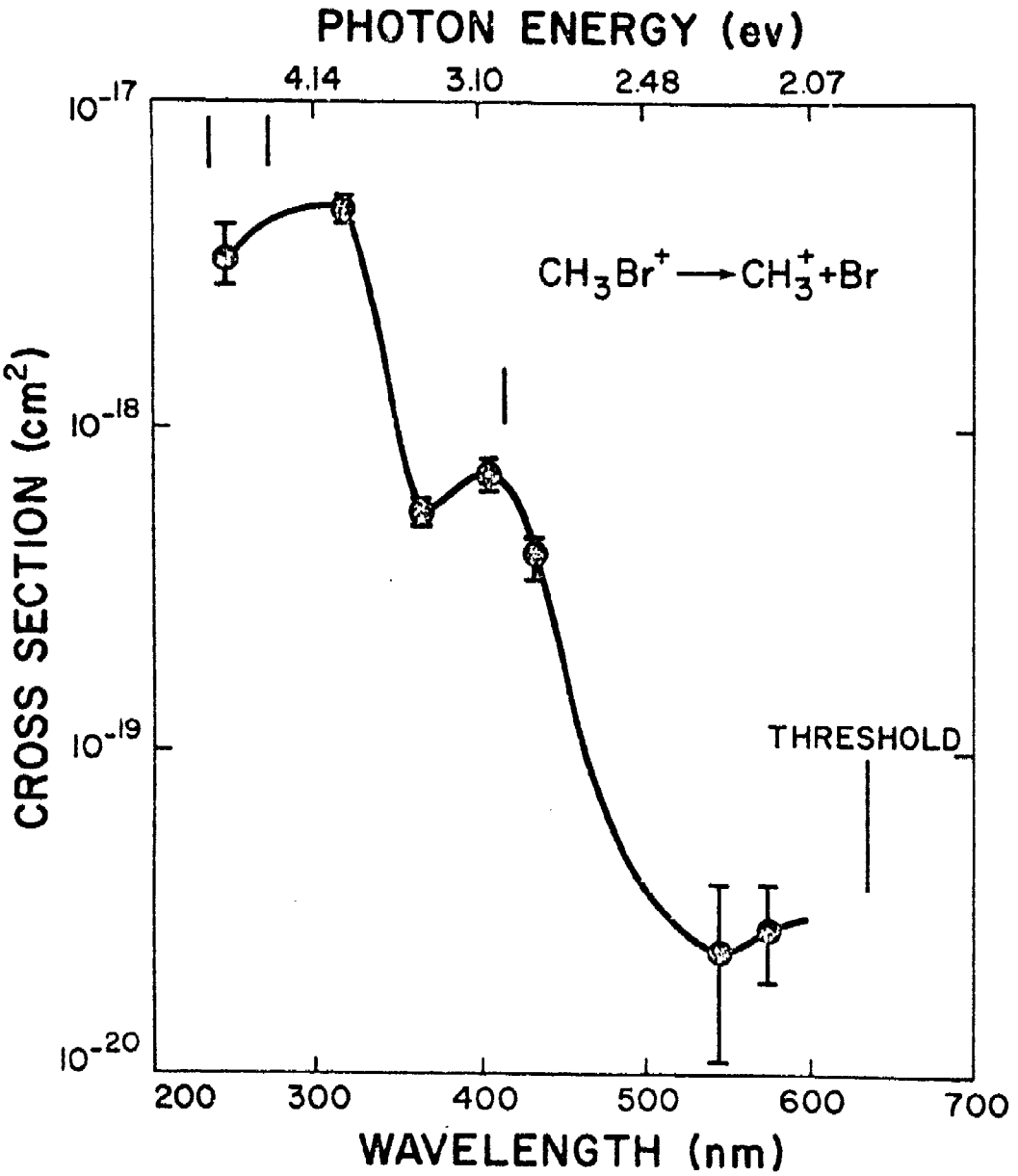

Fig. 6. Experimental results for the photodissociation of CH_3Br^+. See caption, Fig. 5. for additional explanation.

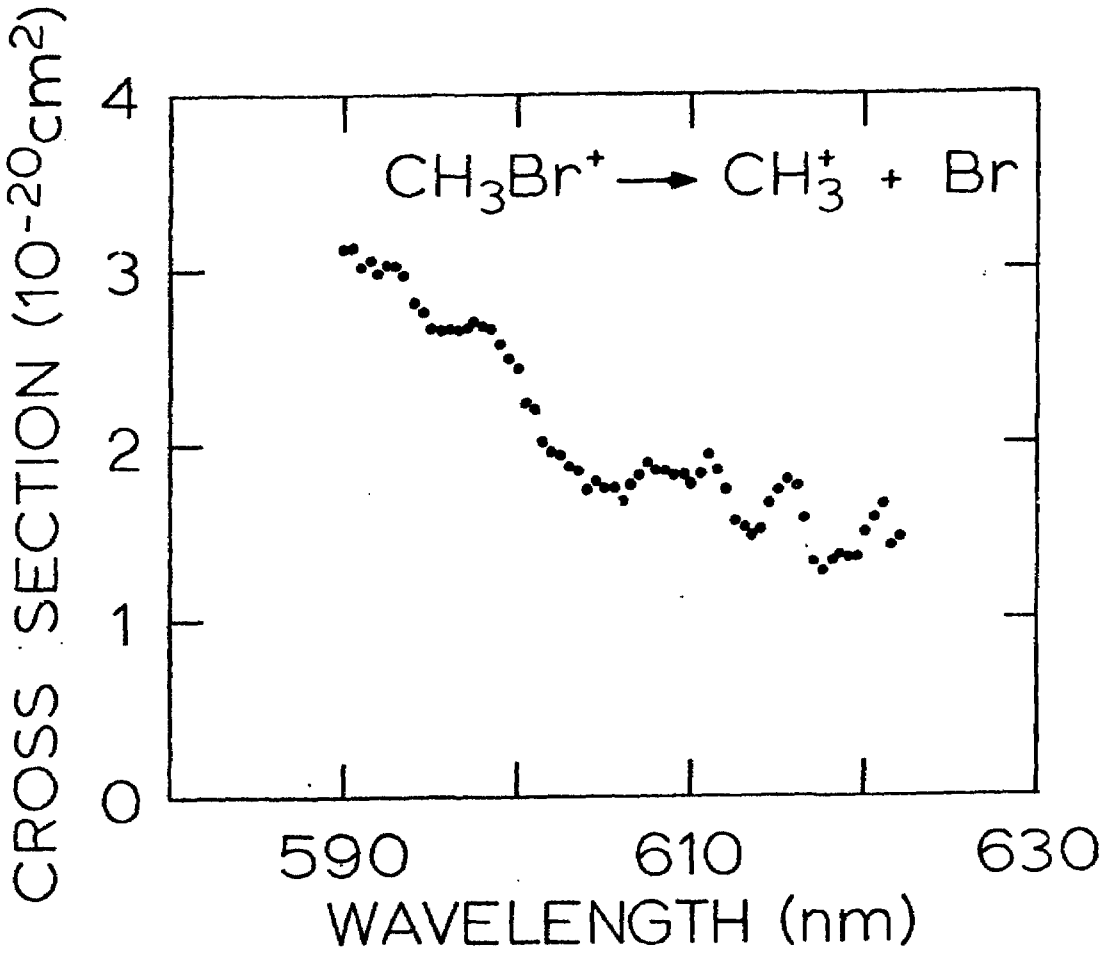

Fig. 7. High resolution data on the photodissociation of CH_3Br^+ obtained using the tunable dye laser with Rhodamine 6G.

using the Hg lamp are summarized in Table II. The threshold for the reaction appears to occur between 435 and 405 nm giving a bond dissociation energy for SF_6^- of 2.95 ± 0.1 eV.

D. Negative Ions in Carbon Dioxide

In pure CO_2 the CO_3^- ion is produced by dissociative attachment

$$e^- + CO_2 \rightarrow CO + O^- \qquad \text{(R17)}$$

followed by three body association

$$O^- + 2CO_2 \rightarrow CO_3^- + CO_2 \qquad \text{(R18)}$$

Rate coefficients for reaction (R18) have been reported in the range from 9×10^{-29} to 1×10^{-27} cm^6/sec at room temperature[22-23] with the more recent results favoring the higher value.

Our measured ratio of CO_3^- current to O^- current as a function of source pressure is given in a logarithmic plot in Figure 8. The source configuration used in this work is estimated to give a mean source residence time for ions of about 10^{-3} second at pressures of ca. 1 torr. The straight line in Figure 8 is calculated assuming a rate coefficient for reaction (R18) of 1×10^{-27} and that the O^- residence time is 10^{-3} sec, independent of pressure. Except at the lowest pressures, where the residence time is expected to be smaller, the experimental results are in good agreement with this calculation. It should be emphasized that reaction (R18) and the corresponding rate coefficient refer to producing stable CO_3^- which is observed in the mass spectrometer; the CO_3^- ions are not necessarily "thermalized" and may contain substantial internal excitation.

TABLE II

Photodissociation Cross Sections For $SF_6^- \rightarrow SF_5^- + F$

λ(nm)	$\sigma(10^{-19} cm^2)$
305	2.0 ± 0.4
365	1.4 ± 0.4
405	0.8 ± 0.4
435	0.35 ± 0.35
550	0.3 ± 0.3
580	<0.3

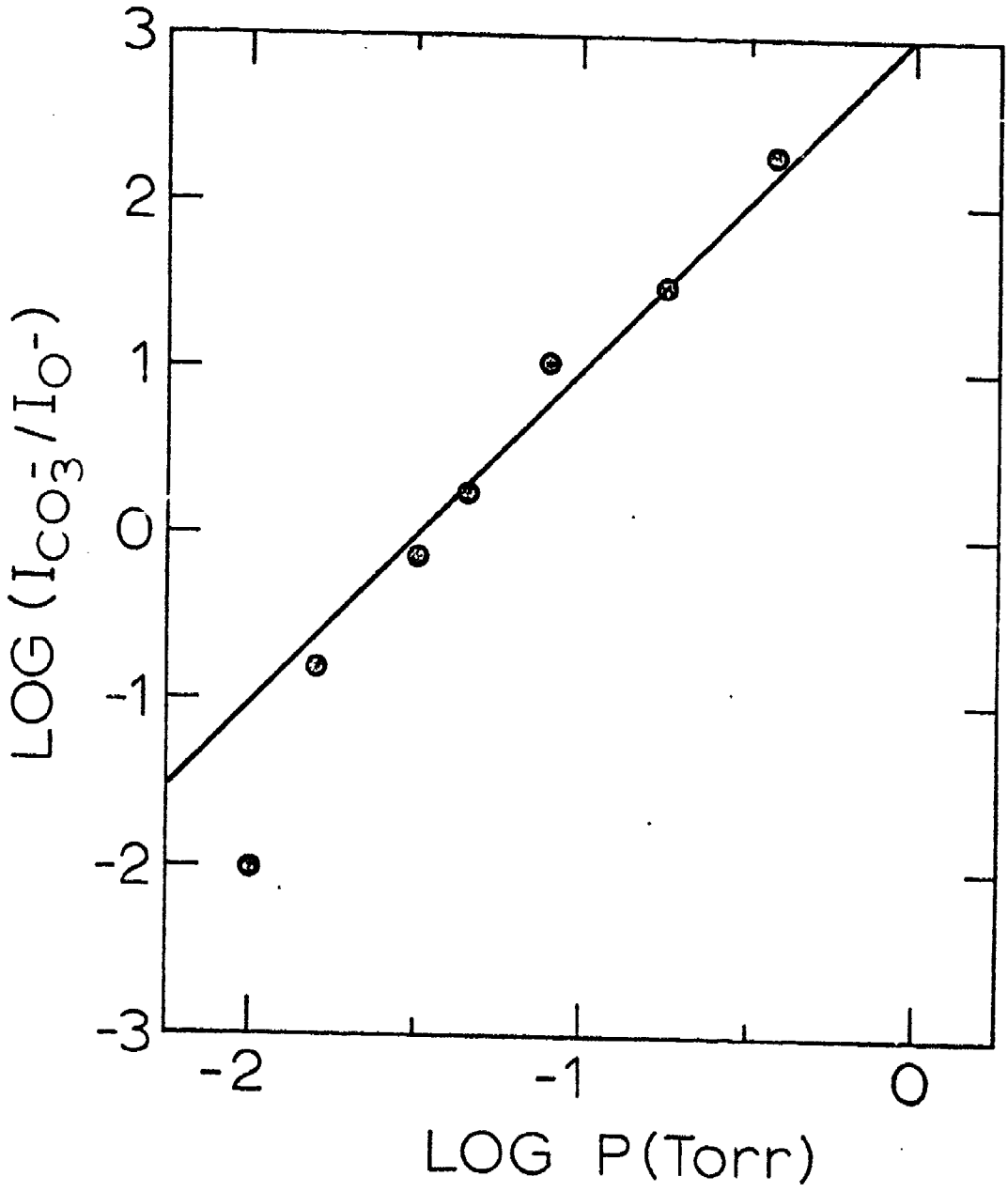

Fig. 8. Logarithmic plot of ration of CO_3^- to O^- current as function of CO_2 pressure in ion source. The straight line corresponds to the steady state ratio for a rate constant for reaction (R18) of 1×10^{-27} cm^6/sec and a source residence time of 10^{-3} sec.

Photodissociation of CO_3^-

The results obtained on reaction (R4) using Rhodamine 6G in the tunable dye laser are summarized in Figure 9. In most of our work we have attempted to obtain "thermalized" reactant ions by operating the ion source at relatively high pressures, ca. 0.5 torr and above, for example, as in curves A-C in Figure 9. Recently Cosby and Moseley[24] have reported an independent study of this reaction which showed structure quite similar to that found in our initial studies but with a significantly larger amplitude to the structure. Also they found absolute cross sections for photo-destruction of CO_3^- which were nearly an order of magnitude larger than our values for photodissociation. In the apparatus used by Cosby and Moseley the absolute cross section for O^- production could not be measured directly; but on the basis of their observation that the relative cross section for O^- production showed a similar structure to that observed for the total photo-destruction they tentatively concluded that photo-dissociation was the major process.

In attempts to resolve the apparent discrepancy between our results and theirs, we extended our measurements to lower pressures, as shown in curves D and E in Figure 9. At lower pressures, ca. 0.1 torr, the amplitude of the observed structure is definitely increased; however, the average cross section in the range between 580 and 620 appears to decrease. A detailed comparision of our lowest pressure result, curve A from Figure 9, with the results of Cosby and Moseley is made in Figure 10. Except for a discrepancy of about 1 nm in the calibration of the wave length scale,[25] the positions and amplitudes of the observed structures are in excellent agreement, but the absolute cross sections differ by about a factor of eight.

We have also studied photodissociation of CO_3^- using the six most intense lines from the super pressure Hg light source. At 305 nm no O^- product was observed giving an upper limit on 5×10^{-20} cm^2 for the cross section. The

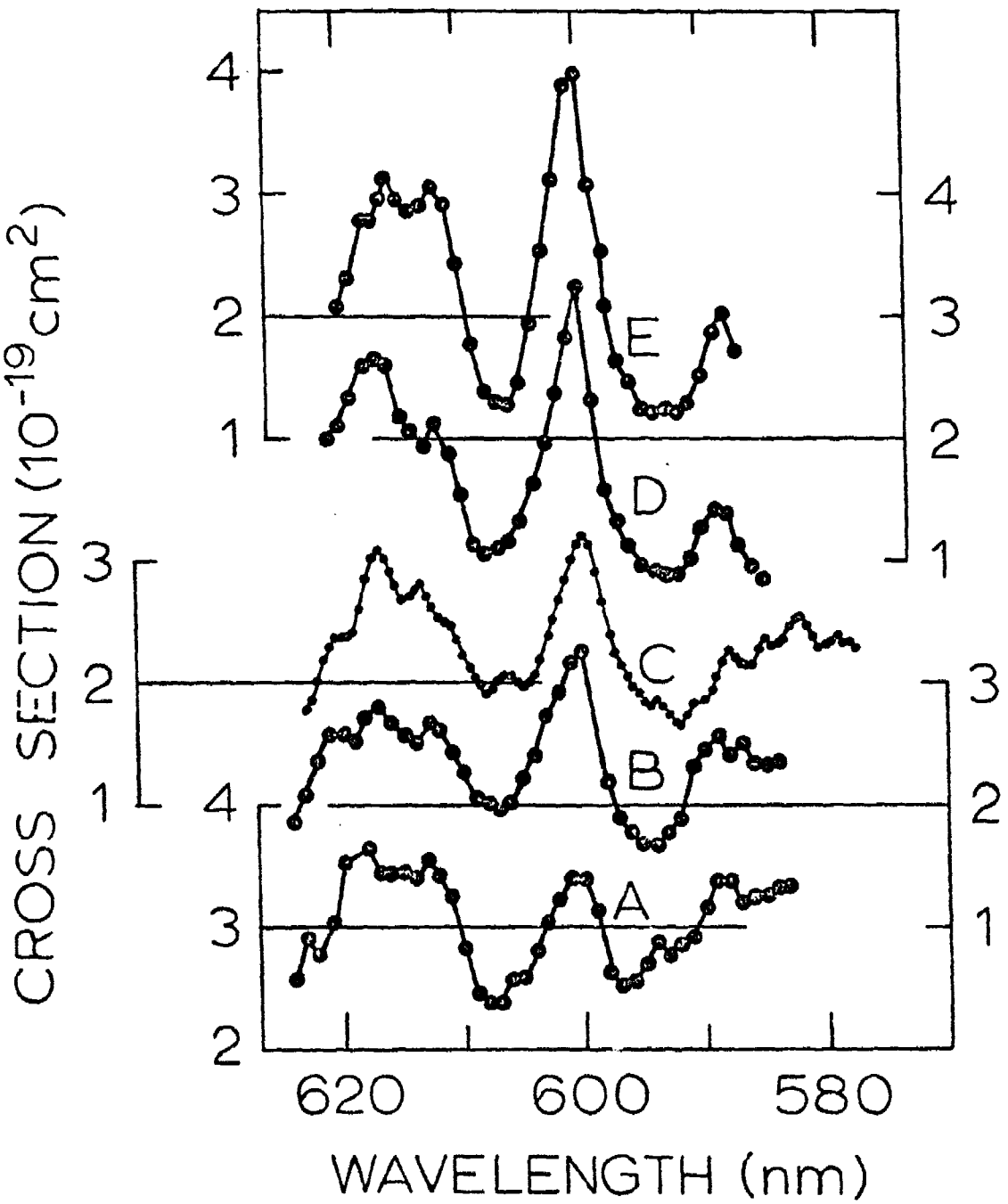

Fig. 9. High resolution data on the photodissociation of CO_3^-, reaction (R4), using the tunable dye laser with Rhodamine 6G obtained at several ion source pressures; A-1.4 torr, B-0.9 torr, C-0.5 torr, D-0.1 torr, E-0.1 torr total with 0.01 torr CO_2 balance air. The correct scale for each result is indicated by the horizontal line through the data.

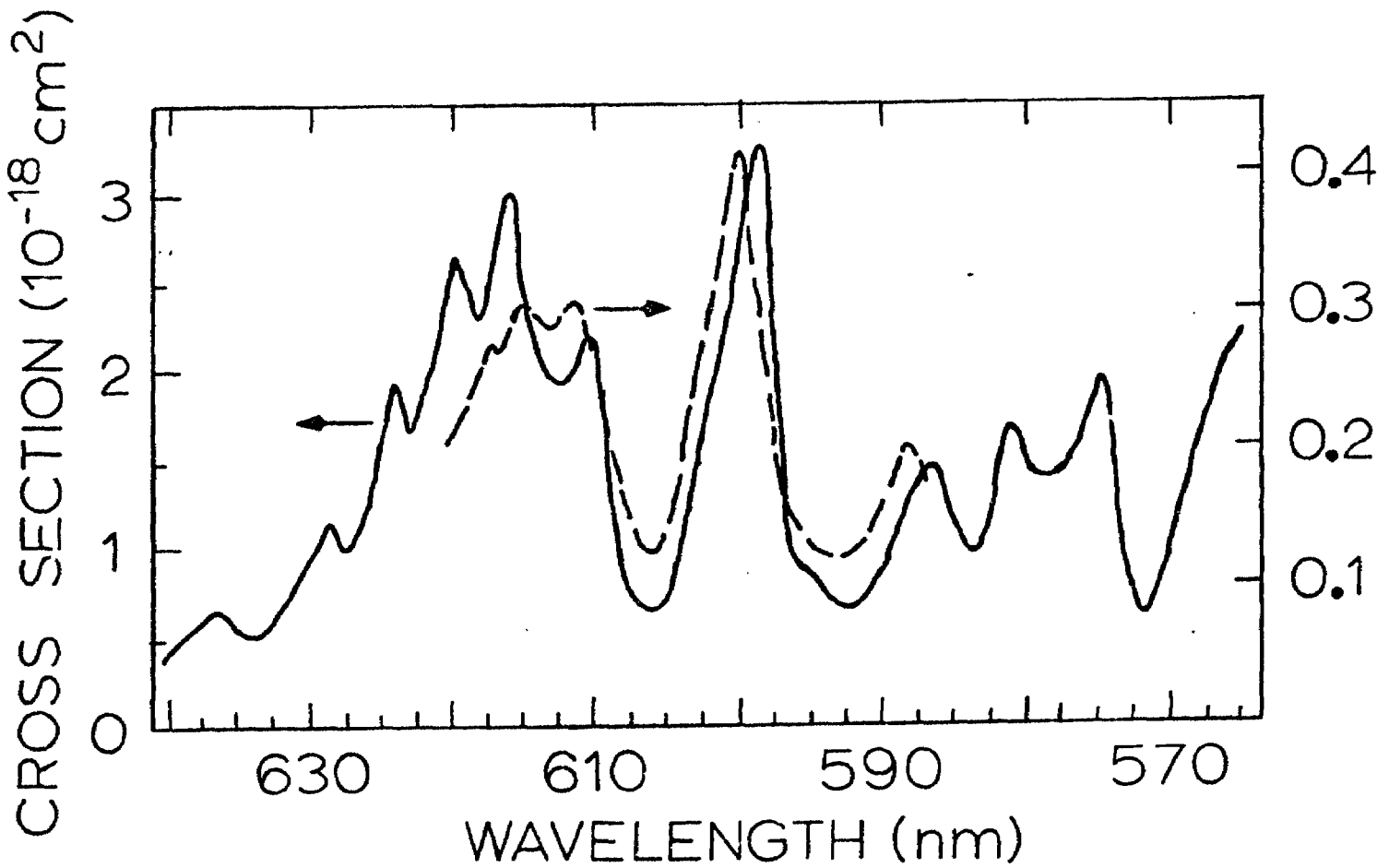

Fig. 10. Comparison of the low pressure results on photodissociation of CO_3^-, curve A from Figure 9, with the photodestruction cross sections reported by Cosby and Moseley, ref. (24). The discrepancy in peak location has been shown to be due to a 1 nm error in the calibration of the wavelength scale of the dye laser used in this work.

cross sections observed are summarized in Table III. At the longer wavelengths a large effect of ion source pressure was observed.

Photo-destruction cross sections for CO_3^- have also been measured by Moseley, et. al.[11] using seven wavelength produced by an argon ion laser in the range between 457.9 and 528.7 nm. They also observed photodissociation at all of the wavelengths studied but the fraction of the total photodestruction due to photodissociation was not determined. These results together with those from reference (24) and the the results of the present work are summarized in Figure 11.

Photodissociation cross sections at 650 nm and 690 nm were measured in this work using Kiton Red S and Cresyl Violet Perchlorate, respectively in the dye laser; these points, labelled C in Figure 11, represent the average of several measurements at the indicated wavelengths but unfortunately sufficiently stable operation of the dye laser was not obtained with these dyes to allow more detailed studies in this wavelength region. Points labelled E and D are the results obtained in this work at high (ca. 1 torr) and low (ca. 0.1 torr), respectively, using the Hg light source. Points labelled G are the total photodestruction cross sections measured by Moseley, et.al.,[11] and points H are the corresponding photodissociation cross sections assuming that all of the observed photodestruction at 458 nm is due to photodissociation. Curve F represents smooth curves drawn through the data of reference (24) ignoring the fine structure which cannot be adequately reproduced on a graph covering this wide wavelength range. Curves A and B are similar smooth curves drawn through the data obtained in this work at 1.4 torr and 0.1 torr and correspond to the data given as curves A and E respectively in Figure 9. The dashed lines indicate possible connections between various sets of data.

The fact that the two sets of data appear to join together smoothly

TABLE III

Photodissociation Cross Sections for the Reaction $CO_3^- \rightarrow O^- + CO_2$

Wavelength(nm)	Cross Section (10^{-19} cm^2) 0.1(1)	1.0(1)
305	<0.5	<0.5
365	1 ± 0.6	1 ± 0.6
405	2 ± 0.3	4 ± 1
435	7 ± 1	13 ± 1.5
550	1 ± 0.5	5.4 ± 0.5
580	0.3 ± 0.1	1.6 ± 0.2

(1) Ion source pressure in torr.

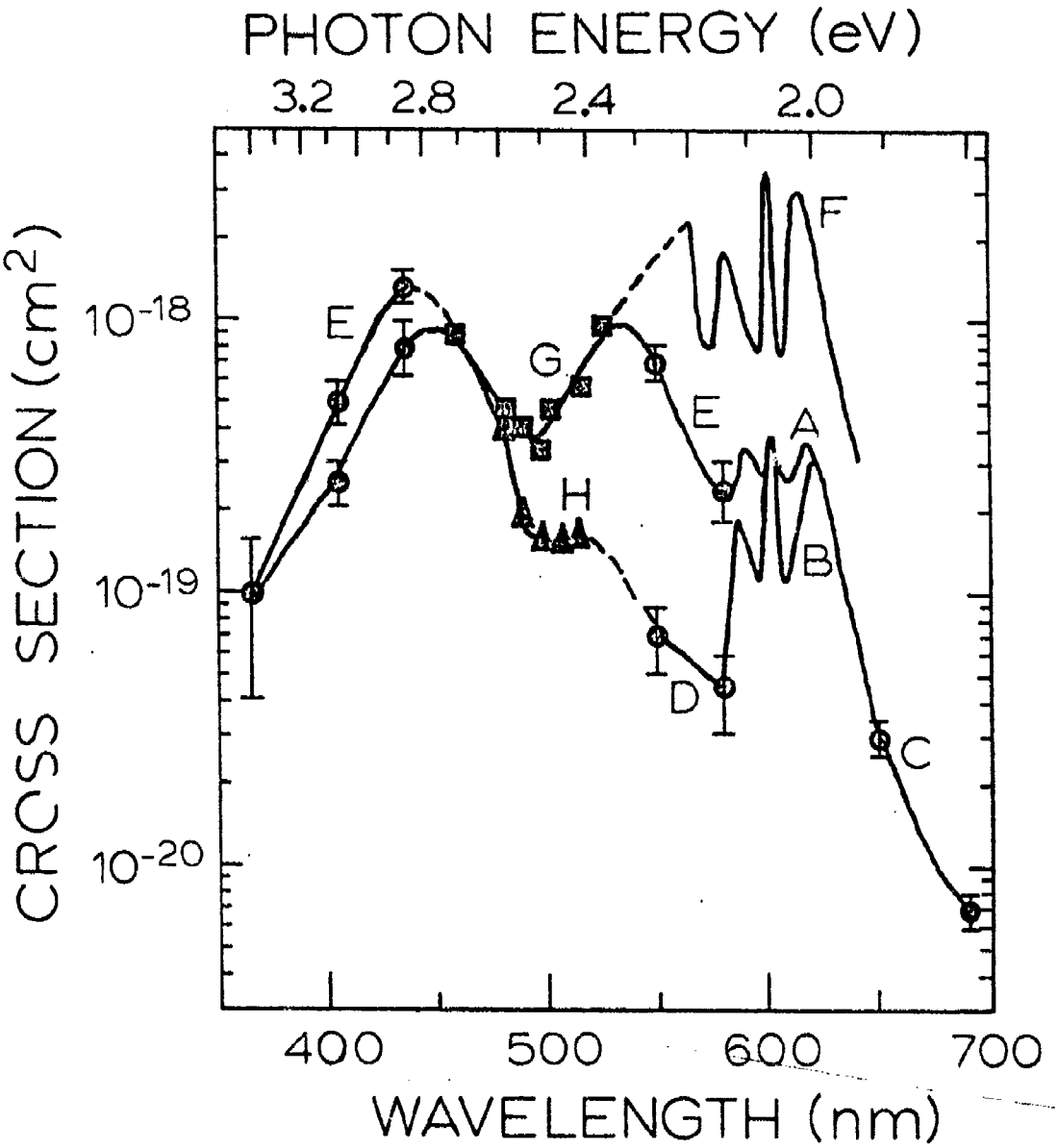

Fig. 11. Summary of results on CO_3^-. This work at 1.4 torr (A) and 0.1 torr (B) using the tunable dye laser with Rhodamine 6G. points (C) obtained using Kiton Red S and Cresyl Violet per chlorate in dye laser at source pressure of 0.5 torr. Data obtained using the H_β lamp, (D) at 0.1 torr, and (E) at 1.0 torr source pressures. (F) and (G) are photodestruction cross sections from refs. (24) and (11), respectively. Points (H) are the relative photodissociation cross sections from ref. (11) plotted assumming that all of the photodestruction observed at 458 nm is due to photodissociation.

between 435 and 458 nm seems to suggest that the large difference in absolute cross sections observed at longer wave lengths are probably not primarily due to any systematic differences in techniques for determining absolute cross sections in the two experiments. This conclusion is further supported by the fact that cross sections for the reaction

$$O_3^- \xrightarrow{h\nu} O^- + O_2 \qquad \text{(R12)}$$

recently measured in the 600 nm range using our apparatus are in good agreement with those reported by Cosby et al.[12]

Discussion

Only a tentative, highly speculative, explanation of the above observations is possible at present. Clearly, high resolution data over the entire visible spectrum together with identification of all of the products and measurement of their kinetic energies is required to develop a complete understanding of this complex system.

The large variation of the photodissociation cross section with ion source pressure strongly suggests that the internal energy of the CO_3^- is slowly decreased by collisions with CO_2. The CO_3^- ions are initially formed by the highly exoergic reaction

$$O^- + CO_2 \rightarrow (CO_3^-)^* \qquad \text{(R19)}$$

followed by collisional stabilization. While a single collision may be sufficient to relax the $(CO_3^-)^*$ to below its dissociation limit, we have no prior knowledge of the number of collisions required to "thermalize" the $(CO_3^-)^*$ ions. If the internal energy were only vibrational exciation of the ground electronic state, then fairly rapid relaxation by vibational-vibrational transfer with CO_2 would be expected. However if the ions are initially

formed in excited electronic state (e.g. of different symmetry than the ground state) for which transitions to the ground state are strongly forbidden, then collisional relaxation may be quite slow.

As a first approximation we may assume that the CO_3^- ions may be in either the ground state or a single excited state and that each state has a characteristic photodissociation cross section at a particular photon energy. This is a rather crude approximation since in general we might expect that a rather large number of states might be populated and that the cross section for each may be different. The observed photodissociation cross section is then given by

$$\sigma_{OBS} = f_g\sigma_g + f_u\sigma_u \tag{11}$$

where σ_g and σ_u are the cross sections and f_g and f_u are the fractional populations of the ground and excited states, respectively. If the decay from the excited state to the ground state is entirely due to collisional relaxation, then the pressure dependence of the observed photodissociation cross section is given by

$$\sigma_{OBS} = \sigma_g + (\sigma_u-\sigma_g)\, e^{-\alpha p} \tag{12}$$

where

$$\alpha \approx 3 \times 10^{16}\, k_r t \quad torr^{-1} \tag{13}$$

and k_r is the rate constant for collisional relaxation and t is the mean source residence time for the CO_3^- ions.

Results of studies on the pressure dependence of the photodissociation cross sections at 580, 550, 435, and 405 nm are summarized in Figures 12-14. The experimental results are consistent with the predictions of equation (12). The most extensive series of measurements was performed at 580 nm (Figure 12) where rather long measurement times (up to 10^4 seconds) were employed to

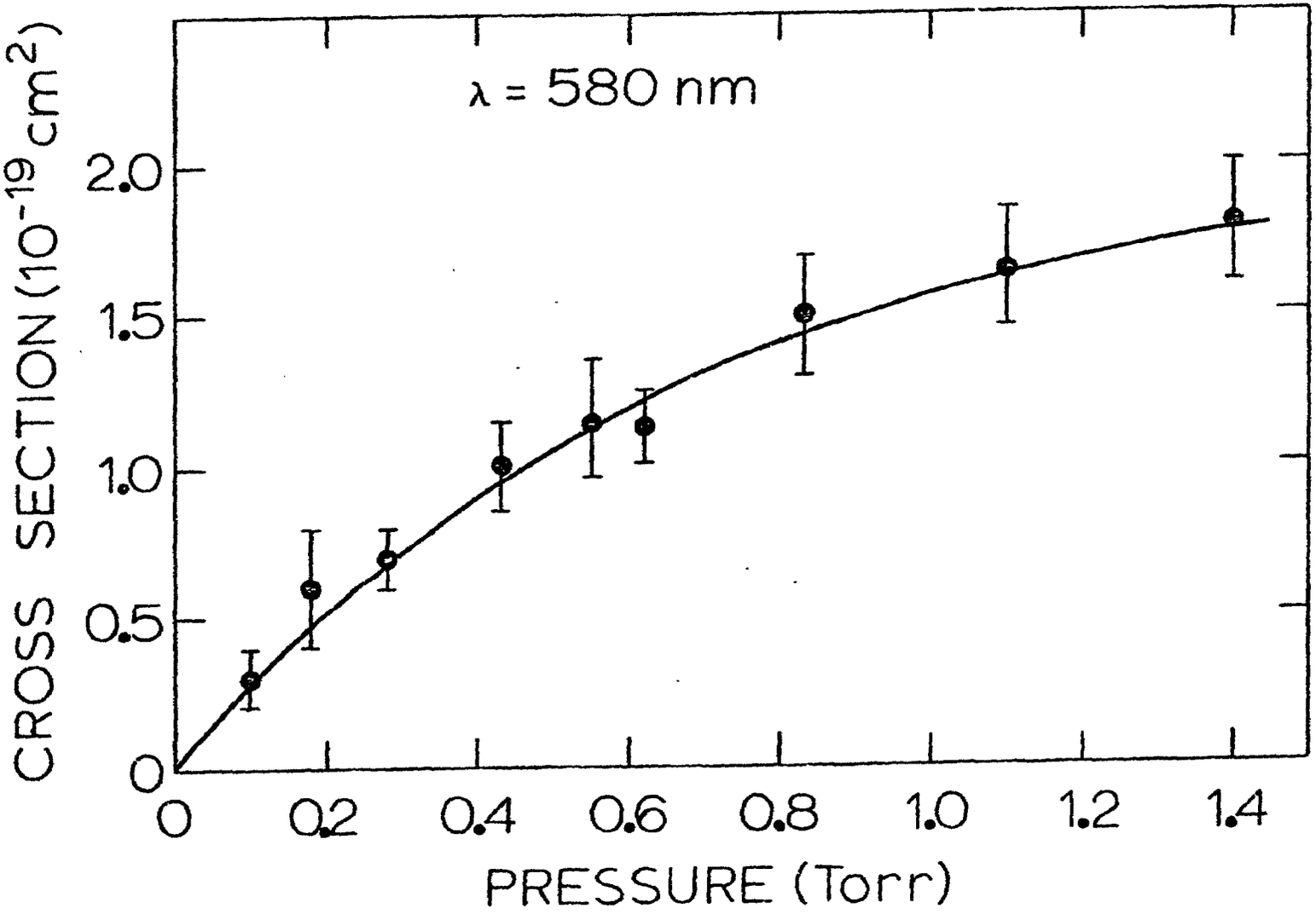

Fig. 12. Photodissociation cross sections for CO_3^- at 580 nm as a function of CO_2 pressure in the ion source.

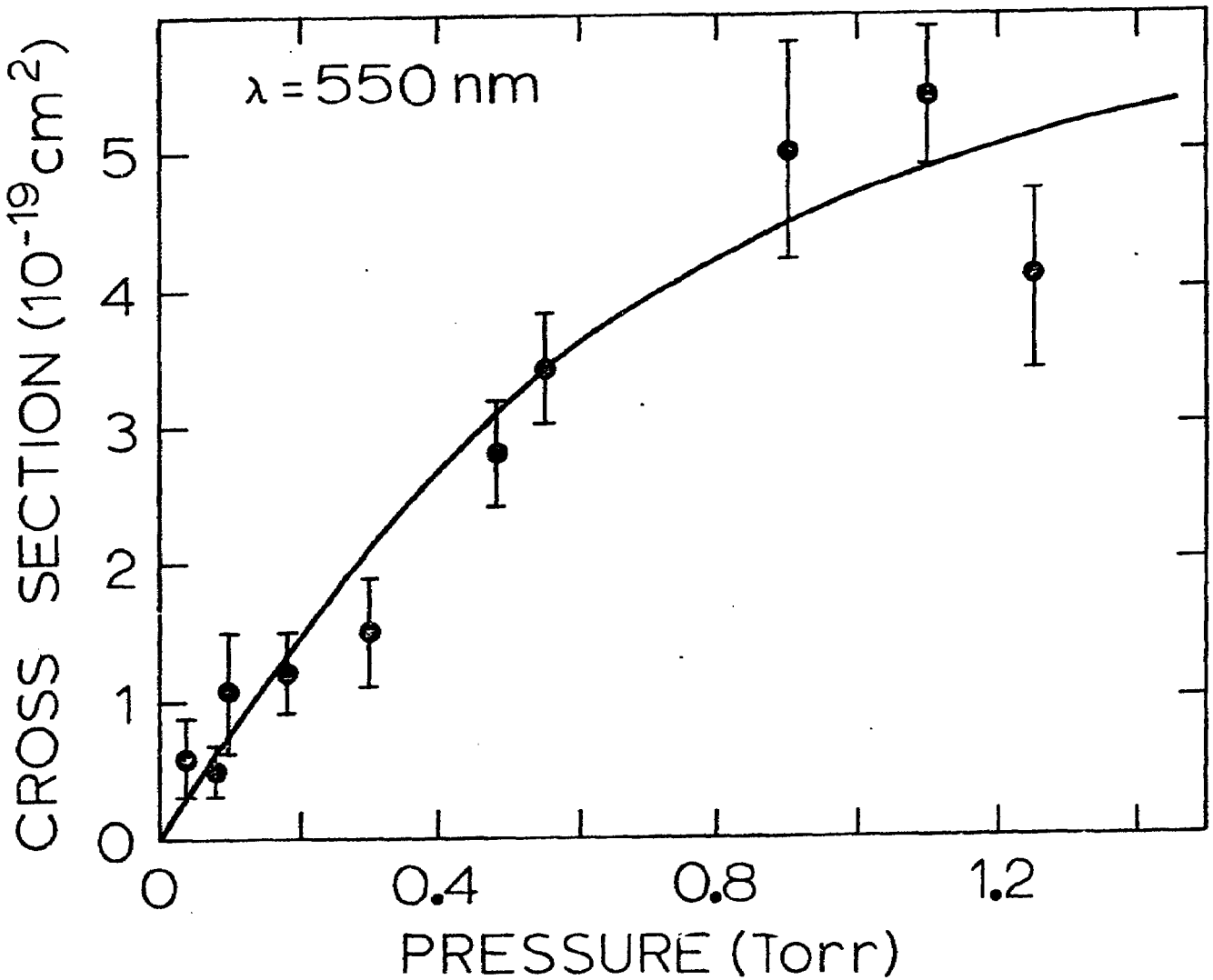

Fig. 13. Photodissociation cross sections for CO_3^- at 550 nm as a function of CO_2 pressure in the ion source.

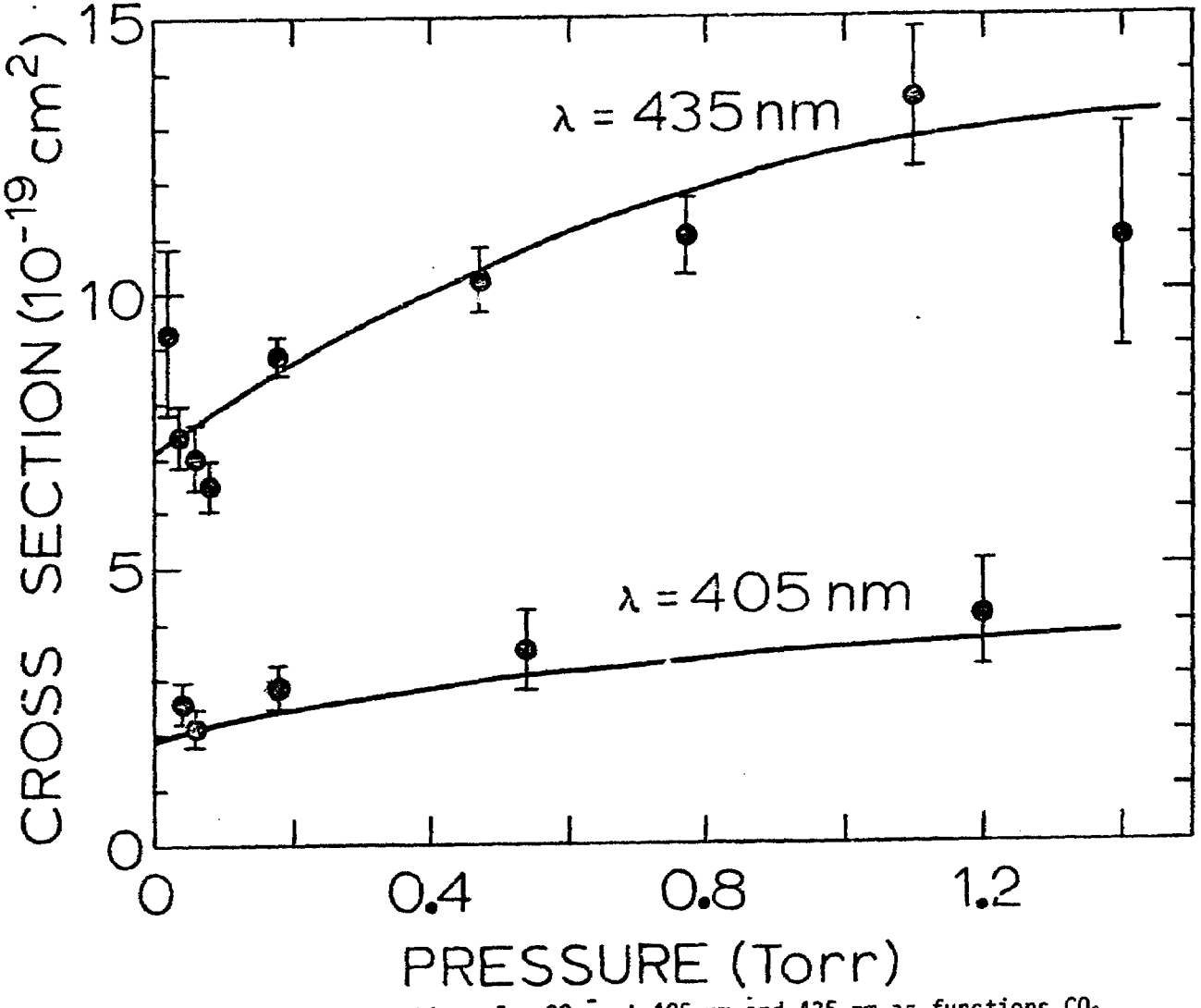

Fig. 14. Photodissociation cross sections for CO_3^- at 405 nm and 435 nm as functions CO_2 pressure in the ion source.

obtain satisfactory precision. The curve was calculated using equation (2) and adjusting the parameters σ_g, σ_u, and k_r until a good fit to the experimental points was obtained.

At 580 nm the values obtained are $k_r = 5 \times 10^{-14}$ cm^3/sec, $\sigma_g = 2 \times 10^{-19}$ cm^2, and $\sigma_u = 0$, assuming a source residence time, t, of 10^{-3} sec. A good fit to the data obtained at the other wavelengths was obtained using the same value of k_r but different values of σ_g and σ_u. At both 580 and 550 nm the best value of the cross section for the excited state was essentially zero giving an upper limit, as determined from the precision of the data, of about 3×10^{-20} cm^2. At both 435 and 405 nm the value determined for σ_u is about one-half of the value for σ_g.

These results indicate that the CO_3^- ions are initially formed in an excited state (or states) which is slowly relaxed ($k_r = 5 \times 10^{-14}$ cm^3/sec) to the ground state. The highly structured photodestruction and photodissociation data observed in the 600 nm band is apparently due to transitions from this state to a second excited state.

The amplitude of the observed structure in the plots of photodissociation cross section versus wavelength in the vicinity of 600 nm is greatly reduced as the source pressure is increased, suggesting that most of the structure can be attributed to transitions from the excited state, but the fact that the average cross section in this region increases with pressure indicates that photodissociation from the ground state is also occurring with a cross section on the order of 2×10^{-19} cm^2.

The difference between the absolute cross sections in the 600 nm band for the photodissociation, as measured in this work, and photodestruction, as measured in the work of Cosby et. al., can be rationalized by assuming that the second excited state is a bound state for which electron detachment and

dissociation are competitive processes. It was pointed out by Cosby and Moseley[24] that if the dissociating state is a trigonal structure of C_{2v} symmetry, as the ground state is believed to be,[26] then an effective barrier to dissociation to linear, ground-state CO_2 is expected. Such a barrier may account for the fact that the energetically favored process (dissociation) is less probable than detachment. If a barrier exists to the dissociation of trigonal CO_3^- to linear $CO_2 + O^-$, then a similar barrier must exist for the reverse reaction by which CO_3^- is formed in the ion source. Thus the CO_3^- ions may be formed initially in the linear configuration for which no such barrier should exist. While vibrational relaxation of the linear configuration by collisions may be quite rapid, relaxation to the ground state trigonal configuration could be quite slow. We tentatively suggest, therefore, that the slow relaxation process observed in this work may correspond to collisional relaxation from the linear configuration to the ground state trigonal configuration.

Energetics

The rapid decrease in the photodissociation cross section between 620 and 690 nm indicates that the true threshold for the transition from ground state CO_3^- to ground states of $CO_2 + O^-$ probably lies somewhere in this region, giving, $\Delta H_0^0 (CO_3^- \rightarrow CO_2 + O^-) = 1.9 \pm 0.1$ eV. A small, but definitely non-zero, cross section was observed at 690 nm ($7 \pm 1 \times 10^{-21}$ cm^2), but this could easily be due to a small fraction CO_3^- with some vibrational excitation. More detailed measurements of the threshold region as a function of pressure and temperature, together with measurements of fragment kinetic energies will be required to accurately determine the true thermochemical threshold. The heat of formation of CO_3 neutral is $\Delta H_f^0 (CO_3) = -43 \pm 5$ kcal/mole $= -1.86 \pm 0.22$ eV,[27] which together with our value for the dissociation energy of CO_3^- implies that the electron affinity of CO_3 is 3.0 ± 0.25 which is in good

agreement with the value of Ferguson et. al.[28]

inferred from the equilibrium constant for the reaction

$$O_3^- + CO_2 \rightleftarrows CO_3^- + O_2 \qquad \text{(R20)}$$

The fact that photodetachment from the excited state is apparently occurring at photon energies of ca. 2 eV in the measurements of Cosby and Moseley suggests that the excited (linear?) configuration lies 1.0 ± 0.25 eV above the ground state.

The rapid decrease in photodissociation cross sections at wavelengths shorter than 435 nm (2.9 eV) may correspond to the onset of photodetachment ·urring as a result of transitions from the ground state, since large photodestruction cross sections in the UV have been observed previously.[29]

Photodissociation of CO_4^-

In mixtures of CO_2 and O_2 the major negative ion formed is CO_4^- presumably through the three-body association of O_2^- with CO_2. Photodissociation of CO_4^- via the reactions

$$CO_4^- \xrightarrow{h\nu} O_2^- + CO_2 \qquad \text{(R5)}$$

$$CO_4^- \xrightarrow{h\nu} CO_3^- + O \qquad \text{(R6)}$$

was observed in this work at wavelengths in the UV. We also looked for the reaction

$$CO_4^- \xrightarrow{h\nu} O^- + CO_3 \qquad \text{(R21)}$$

but no O^- product was observed. The results obtained on the photodissociation of CO_4^- are summarized in Table IV. The observed threshold for dissociation of CO_3^- implies that $\Delta H_f^0 (CO_3^-) = 4.93 \pm 0.1$ eV. Onset of the reaction (R6) occurs between 405 nm and 365 nm which implies a threshold energy of 3.25 ± 0.15 eV. This leads to $\Delta H_f^0 (CO_4^-) = 5.6 \pm 0.2$ eV. The thermochemical threshold

TABLE IV

Photodissociation Cross Sections for the Reactions

$CO_4^- \rightarrow O_2^- + CO_2$ and $CO_4^- \rightarrow CO_3^- + O$

Wavelength(nm)	Cross Section (10^{-19} cm^2) O_2^-	CO_3^-
305	1.4 ± 0.7	1.4 ± 0.1
365	1.0 ± 0.4	0.17 ± 0.04
405	1.0 ± 0.7	<0.1
530	0.7 ± 0.4	<0.1
580	<0.6	<0.1
600	<0.1	<0.1

for reaction (R5) producing O_2^- is then 1.1 ± 0.2 eV. The fact that this reaction apparently does not occur with appreciable cross section at the visible wavelengths investigated may imply that dissociative detachment

$$CO_4^- \xrightarrow{h\nu} O_2 + CO_2 + e^- \qquad \text{(R22)}$$

is the predominant process at longer wavelengths.

E. Positive Ions in Oxygen

The positive ions produced with pure O_2 in the source (50°C) are O^+, O_2^+, O_3^+, and O_4^+. The relative intensities and total ion currents measured as a function of source pressure are given in Table V. We have studied the photodissociation of all three molecular ions.

The O^+ and O_2^+ ions are formed directly by electron impact on O_2. The O^+ may be formed in the ^4S ground state, and the ^2D, and possibly the ^2P, excited states.[30] The O_2^+ may be formed in the $X^3\Sigma_g^-$ ground state as well as the $a^4\Pi_u$, $A^2\Pi_u$, $b^4\Sigma_g^-$, and possibly some higher states. All of the identified states have been well-characterized by spectroscopy;[31] and Franck-Condon factors have been calculated[32] which are in good agreement with the observed photo-electron spectra.[33]

O_3^+ may be formed either by the three body association reaction

$$O^+ + 2O_2 \rightarrow O_3^+ + O_2 \qquad \text{(R23)}$$

or by

$$(O_2^+)^* + O_2 \rightarrow O_3^+ + O \qquad \text{(R24)}$$

where the $(O_2^+)^*$ must be excited to the fourth vibrational level of the $a^4\Pi_u$ state, or above, for this reaction to be exoergic.

Three low-lying electronic states of O_3^+ are observed in the photo-electron

TABLE V

Positive Ions in Oxygen as Function of Source Pressure

Pressure (torr)	Relative Intensity(%) O^+	O_2^+	O_3^+	O_4^+	Total Ion (Amp) Current	$Io_3+/Io+$
0.001	26	74	--	--	5×10^{-12}	~0
0.003	19	82	--	--	5×10^{-11}	~0
0.009	9.8	90	0.15	0.02	5×10^{-10}	.015
0.045	9.0	90.4	0.40	0.13	1.7×10^{-9}	.044
0.07	8.3	91.4	0.34	0.17	4.9×10^{-9}	.041
0.13	5.6	94.0	0.19	0.19	8.0×10^{-9}	.034
0.28	4.5	95.1	0.07	0.18	1.2×10^{-8}	.016
0.40	3.0	96.5	0.06	0.18	8.3×10^{-9}	.018
0.60	2.1	97.6	0.05	0.18	7.2×10^{-9}	.022
1.0	1.4	98.2	0.03	0.34	3.9×10^{-9}	.020

spectra of O_3.[34] Recent CI calculations by Hay, Dunning, and Goddard[35] predict states at energies close to those found in the photo-electron spectra. In addition the theoretical calculations predict four more low-lying states of O_3^+. Since these states involve the removal of one electron and the excitation of a second electron, these states are not observed in the photo-electron spectra.

The O_4^+ dimer is formed by the three body association reaction

$$O_2^+ + 2O_2 \rightarrow O_4^+ + O_2 \qquad \text{(R25)}$$

Conway et. al.[36] have reported a value of the dissociation energy of O_4^+ of 0.48 eV which accounts for the rather low intensities of O_4^+ obtained at 50° C ion source temperature.

Photodissociation of O_2^+

Photodissociation of O_2^+ was observed using the laser with Rhodamine 6G. Results obtained in the 585 to 620 nm band at a source pressure of 0.02 torr are given in Figure 15. While there appears to be clear evidence of some structure in the observed variation of cross section with wavelength, the data is not sufficient to identify the transition involved. However, the fact that photodissociation is observed at these low energies clearly shows that a significant fraction of the O_2^+ ions are in excited states. Figure 16 shows the results of a study of the collisional relaxation of $(O_2^+)^*$. This semi-logarithmic plot of photodissociation cross section vs. source pressure appears to have two linear segments. Assuming a source residence time of 10^{-3} sec, these segments correspond to relaxation rate constants of 1.7×10^{-12} and 1.7×10^{-13} cm^3/sec, respectively. There are three known states of O_2^+ which could be photodissociated at the photon energies used; however, since radiation from the $A^2\Pi_u$ state to the $X^2\Sigma_g^-$ ground state is allowed, this state

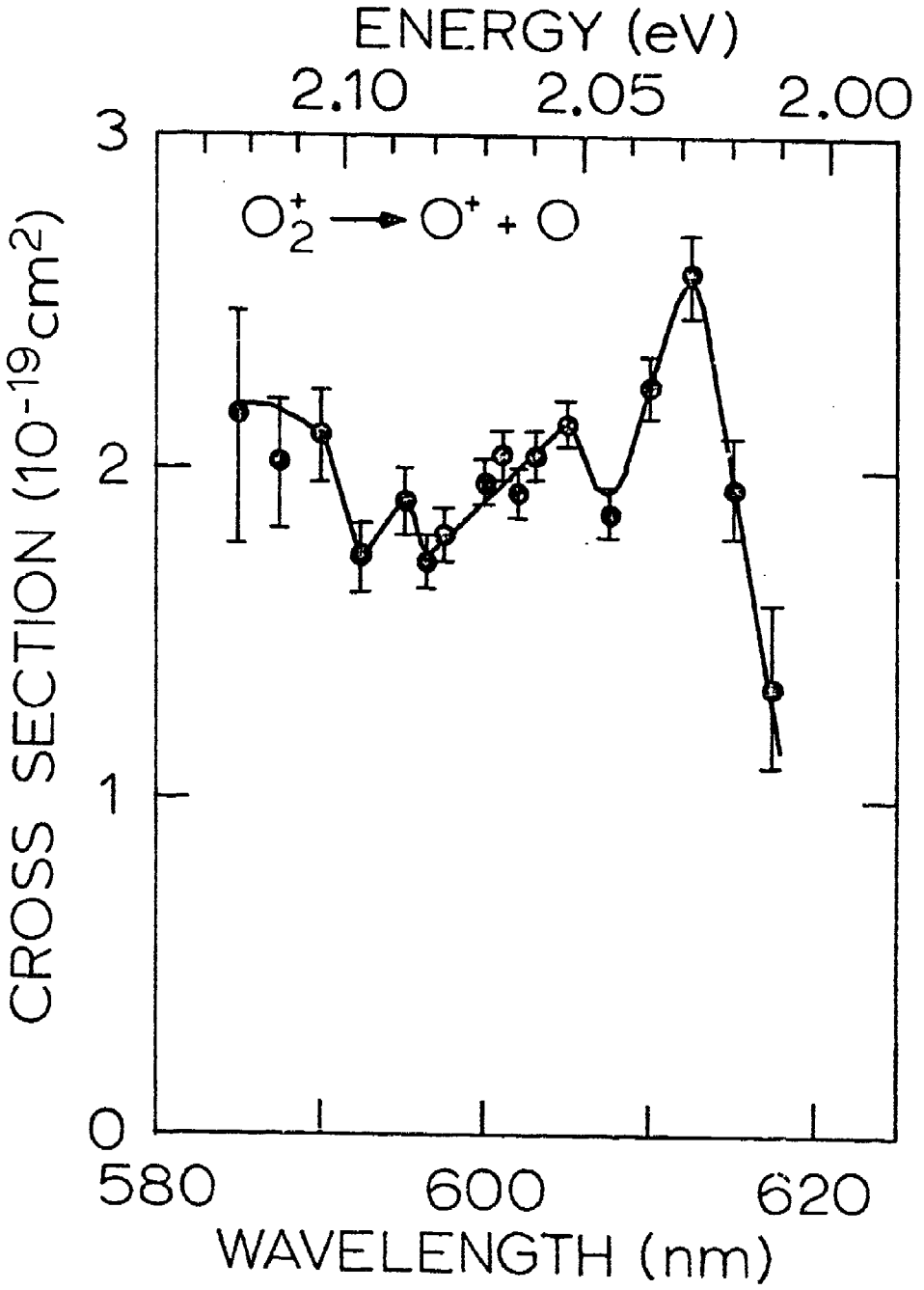

Fig. 15. Photodissociation cross sections for O_2^+ at 0.02 torr source pressure using the tunable dye laser with Rhodamine 6G.

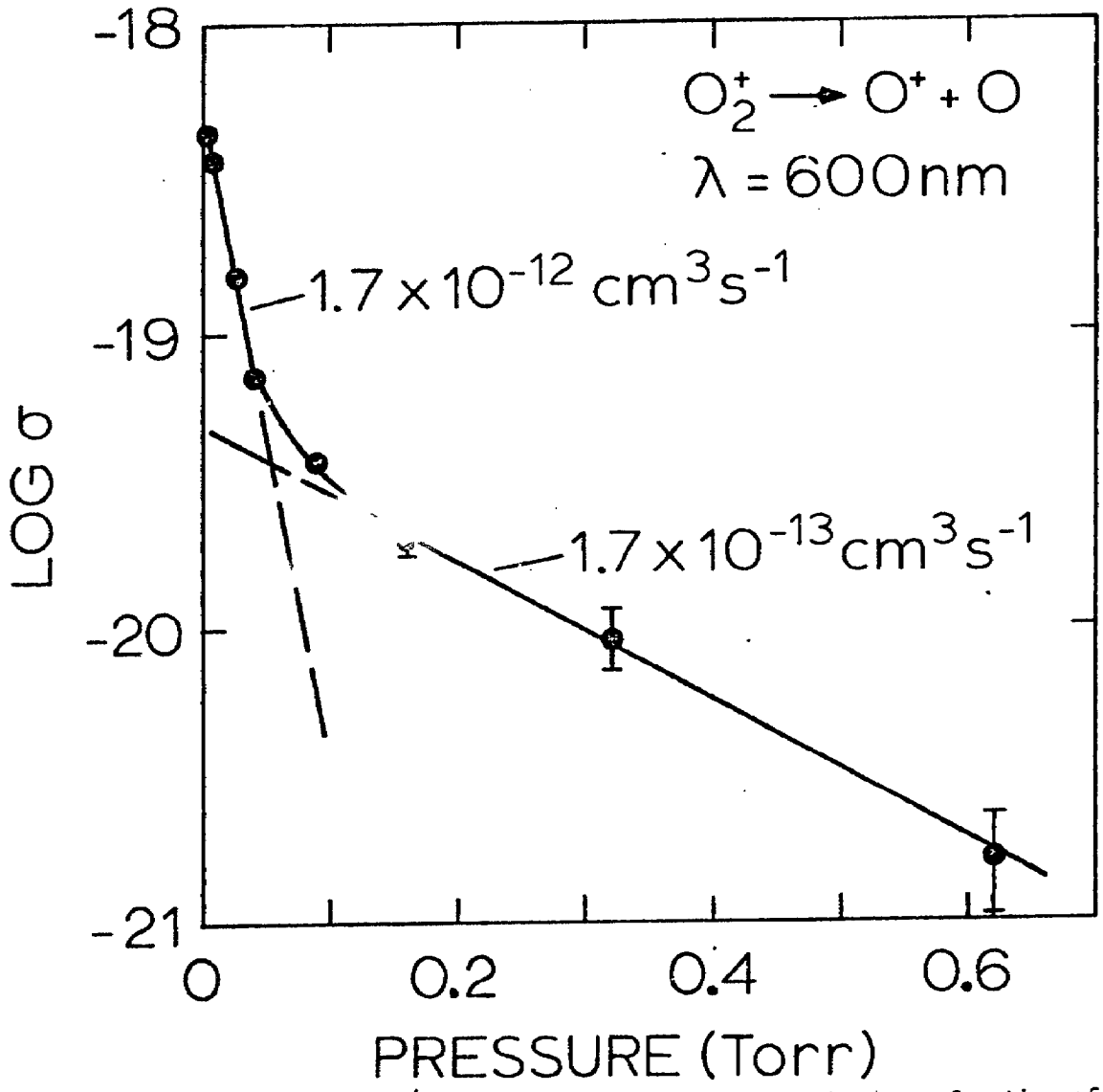

Fig. 16. Semi-logarithmic plot of the O_2^+ photodissociation cross section as a function of ion source pressure.

is probably relaxed rapidly by radiation. This leaves the $a^4\Pi_u$ state ($v \geq 5$) and the $b^4\Sigma_g^-$ states as potential candidates for the observed states. It appears that the relatively fast relaxation observed may correspond to vibrational relaxation of the $a^4\Pi_u$ to below $v = 5$, while the slower process may correspond to collisional relaxation of the $b^4\Sigma_g^-$ electronic state. Additional measurements covering a somewhat wider range of wavelengths should allow the unambiguous identification of the states involved.

Photodissociation of O_3^+

For ground state O_3^+ dissociations to $O^+ + O_2$ and to $O_2^+ + O$ are endoergic by 2.2 and 0.6 eV, respectively. Thus it was rather surprising to observe that photodissociation of O_3^+ at 600 nm (2.07 eV) leads predominately to production to O^+ with a large cross section. Measured cross sections for both photodissociation process is summarized in Table VI for several wavelengths between 305 and 760 nm. In the UV the measured cross sections for the two processes are comparable; but in the visible spectrum, production of O^+ is predominant. On the other hand, collisional dissociation of O_3^+ leads almost exclusively to production of O_2^+.

The results of a detailed examination of the wavelength dependence of the cross section for the reaction $O_3^+ \rightarrow O^+ + O_2$ in the 580 to 620 nm band are given in Figure 17. The main feature apparent is a series of three steps corresponding to a spacing of 0.04 eV (320 cm^{-1}) which is a somewhat closer spacing than the vibrational structure found in the photoelectron spectrum of O_3.

The observed dependence of the photodissociation cross section for reaction (R9) over the range from 670 to 305 nm is shown in Figure 18. There is a relatively sharp onset at 670±10 nm (1.80 ± 0.02 eV). The first maximum occurs at 590 nm (2.11 eV) and there is an indication of a second maximum at

TABLE VI

Photodissociation Cross Sections For

$O_3^+ \rightarrow O^+ + O_2$ and $O_3^+ \rightarrow O_2^+ + O$

	$\sigma(10^{-18}\,cm^2)$	
λ(nm)	O^+	O_2^+
305	3.9 ± 1.3	6 ± 2
365	8.3 ± 0.6	8 ± 2
405	10.1 ± 1.2	6 ± 2
435	10.5 ± 0.9	8 ± 2
500	10.0 ± 0.1	(1)
550	12.5 ± 1.0	1.3 ± 1
580	13.5 ± 1.0	1.5 ± 1
590	13.0 ± 0.2	(1)
600	11.6 ± 0.2	2.7 ± 0.3
610	10.5 ± 0.2	(1)
620	9.0 ± 0.3	(1)
635	6.2 ± 0.8	(1)
660	2.8 ± 0.8	(1)
670	<1	(1)

(1) Not measured.

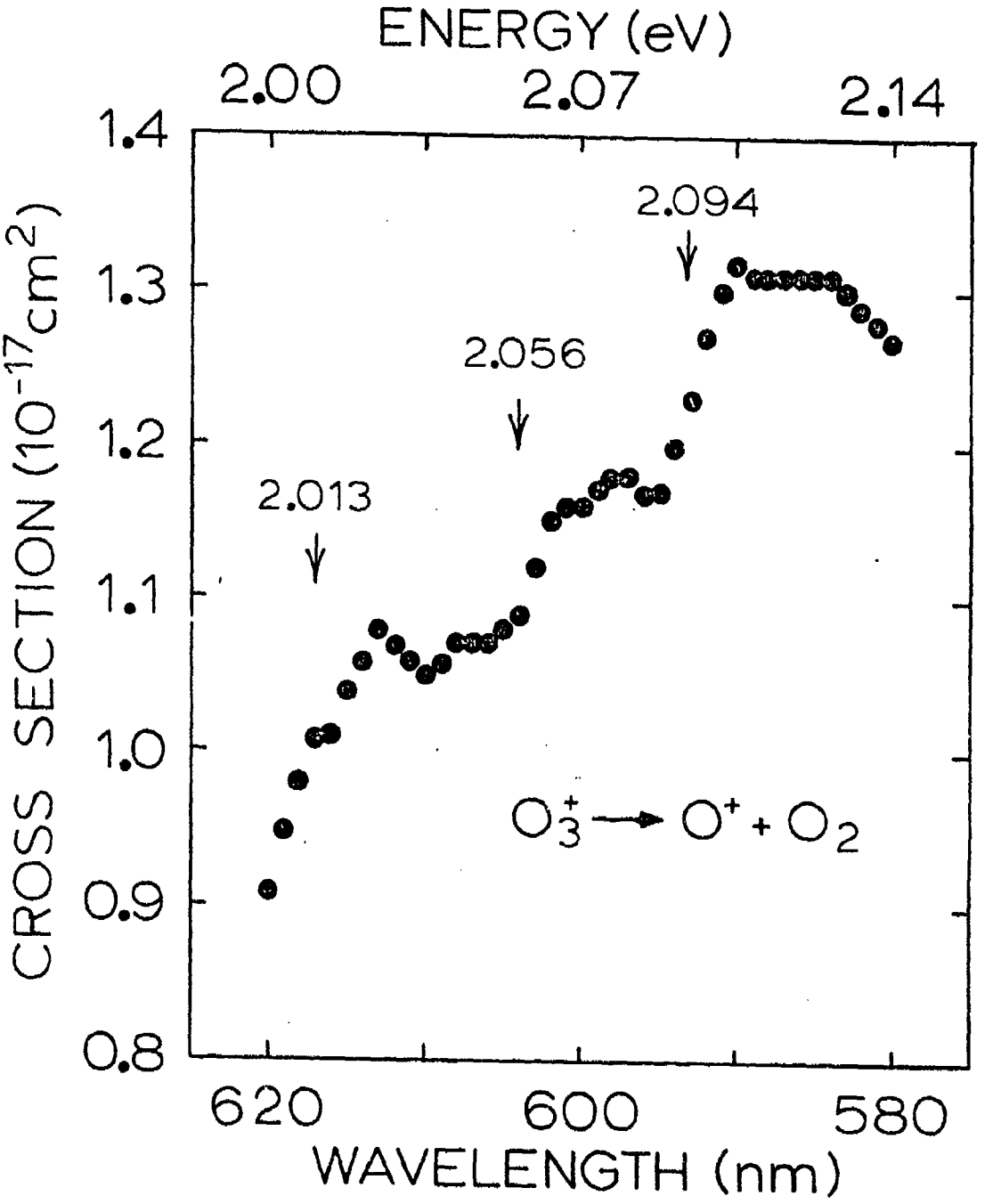

Fig. 17. Photodissociation cross sections for O_3^+ measured using the tunable dye laser with Rhodamine 6G.

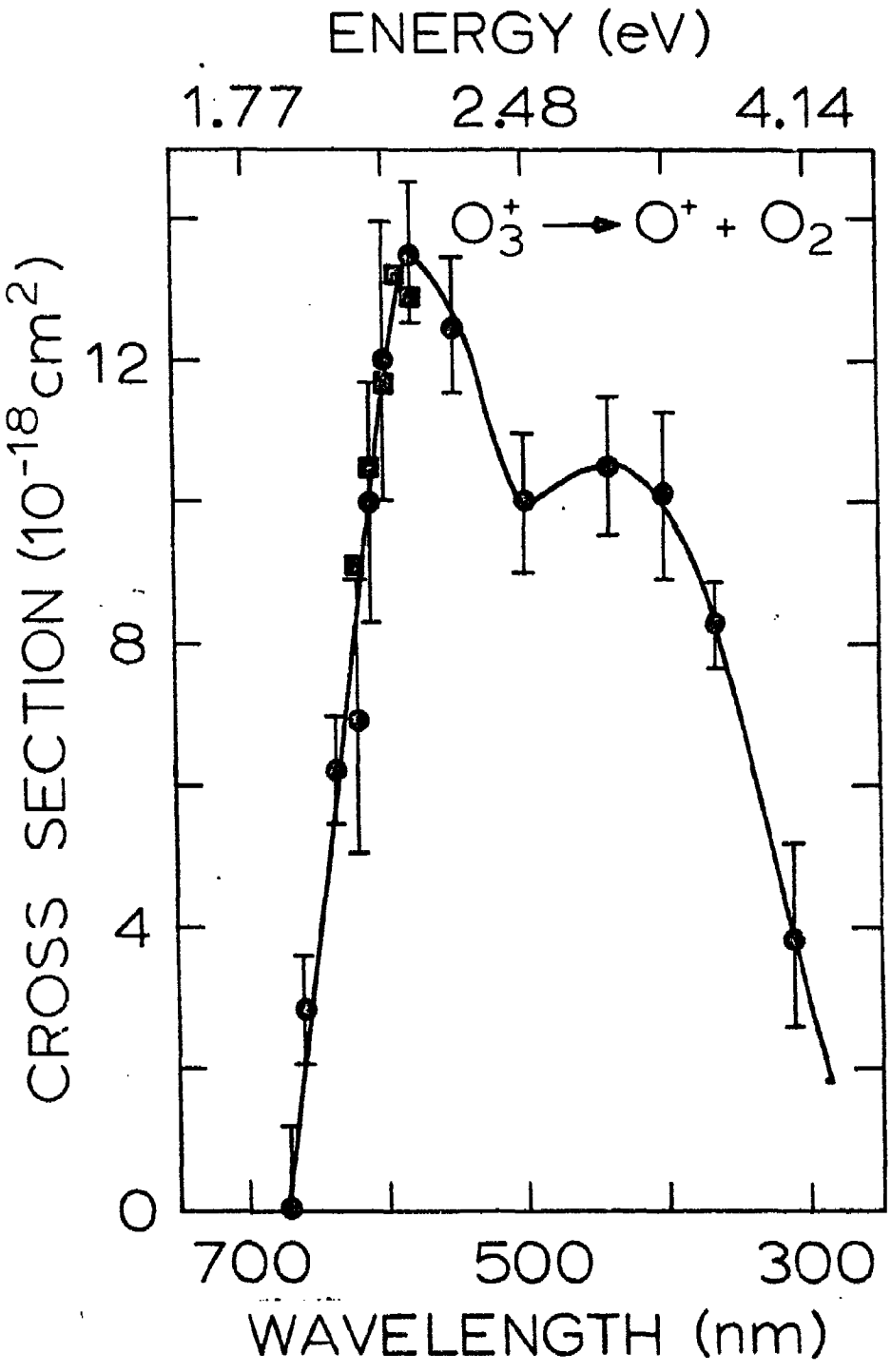

Fig. 18. Photodissociation cross sections for O_3^+, obtained using the Hg lamp, obtained using the dye laser.

about 430 nm (2.9 eV). The cross section at 590 nm is 1.3×10^{-17} cm^2, one of the largest photodissociation cross sections thus far observed in this work, despite the fact that the observed reaction from the ground state of O_3^+ is apparently endoergic by at least 0.1 eV. These results seem to imply that the O_3^+ is formed almost exclusively in an excited state.

The absence of ground state O_3^+ is probably due to the almost exact accidental resonance with the v = 2 level of ground state O_2^+. As a result ground state O_3^+ may be efficiently removed by the charge exchange reaction

$$O_3^+ + O_2 \rightarrow O_2^+ + O_3 \qquad \text{(R26)}$$

This reaction also may be involved in the efficient collisional relaxation of some of the excited states of O_2^+. For example the reaction

$$O_2^+ (a^4\Pi_u) + O_2 \rightarrow O_3^+ (1^2A_1) + O(^3P) \qquad \text{(R27)}$$

is exothermic for the v = 4 level of O_2^+ in the $a^4\Pi_u$ state. The fast relaxation process observed in the photodissociation of O_2^+ may correspond to the machinism consisting of (R27) followed by (R26).

We conclude from our data, the photoelectron spectra,[34] and the calculations of Hay et. al.,[35] that the O_3^+ that we observe is formed mainly in the 1^2B_2 state (13.06 eV above the ground state of O_3)

and that absorption of a ca. 2 eV photon further excites the O_3^+ to the 1^2B_1 state by promotion of an electron from the $4b_2$ orbital to the $2b_1$ orbital. The observed threshold of 1.85 eV is about 0.17 eV above the energy necessary to produce ground state $O^+ + O_2$ from the ground vibrational level of the 1^2B_2 state. This implies, if the above energetics are correct, that a barrier to the dissociation exists and that the excess

energy should appear as translational energy of the dissociation products.

Photodissociation of O_4^+

The collision induced dissociation background for this weakly bound dimer is rather large; as a result we were unable to obtain reliable data using the Hg lamp. Data obtained with the dye laser is given in Figure 19. The rapid increase in cross section between 610 and 620 nm probably indicates that the maximum cross section occurs at wavelengths longer than 620 nm.

F. Negative Ions In Oxygen

The pressure dependence of negative ions produced in "pure" O_2 is summarized in Table VII. In addition to the ions shown in the table some ions due to impurities, in particular Cl^- and Br^-, were also present in low abundance (typically less than 1% of the total negative ion spectrum). The pressure dependence of the O_3^-/O^- ratio is in good agreement with the earlier observation that O_3^- is formed by the three-body association

$$O^- + 2O_2 \rightarrow O_3^- + O_2 \qquad \text{(R28)}$$

with a rate constant of 1×10^{-30} cm^6/sec.

In this work we have studied the photodissociation of O_2^- and O_3^-. The intensity of O_4^- was insufficient for satisfactory measurements since the collision induced background was rather large.

The reaction

$$O_2^- \xrightarrow{h\nu} O^- + O \qquad \text{(R11)}$$

was observed to occur with a cross section of $4.2 \pm 0.5 \times 10^{-19}$ cm^2 at 305 ± 10 nm (4.07 ± 0.07 eV) but was not observed at 365 nm or longer wavelengths,

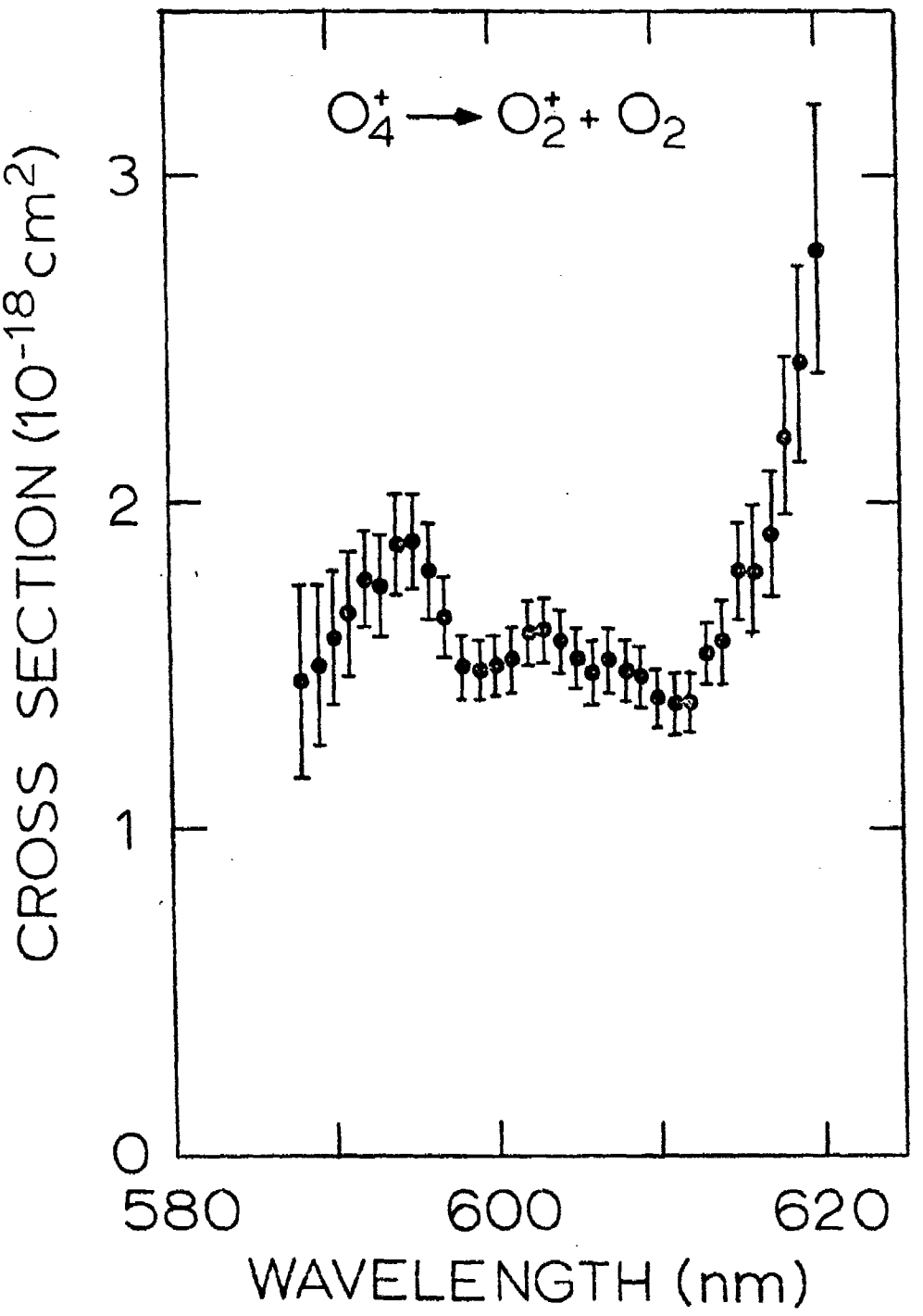

Fig. 19. Photodissociation cross sections for O_4^+ obtained uisng the tunable dye laser with Rhodamine 6G.

TABLE VII

Negative Ions in Oxygen as Function of Source Pressure

Pressure (low)	Relative Intensity (%) O^-	O_2^-	O_3^-	O_4^-	Total Ion Current	$I_{O_3^-}/I_{O^-}$
0.03	69	31	0.1	----	4.35×10^{-10}	1.67×10^{-3}
0.06	75	25	0.3	----	12.7	3.7×10^{-3}
0.09	77	22	1.0	0.02	19.6	1.3×10^{-2}
0.15	74	24	2.3	0.02	14.9	3.1×10^{-2}
0.24	60	37	2.6	0.01	10.8	4.3×10^{-2}
0.36	45	52	2.7	0.01	9.0	6.0×10^{-2}
0.47	33	64	3.0	0.03	8.8	9.1×10^{-2}
0.59	24	73	3.3	0.02	8.3	1.4×10^{-1}
0.76	18	79	3.2	0.14	6.3	1.8×10^{-1}
0.93	12	85	3.2	0.19	4.7	2.7×10^{-1}
1.07	10	87	3.2	0.29	3.5	3.2×10^{-1}

indicating that the maximum cross section at longer wavelengths is less than 1×10^{-19} cm^2. These results are in agreement with the bond dissociation energy of O_2^- of 4.1 eV inferred from the electron affinity of O_2.[37]

Results on the photodissociation of O_3^- are summarized in Figure 20 and Table VIII. The cross section for the reaction

$$O_3^- \xrightarrow{h\nu} O + O_2 \qquad \text{(R12)}$$

obtained at wavelengths between 587 and 620 nm and a source pressure of 0.1 torr and in excellent agreement with the results reported earlier by Cosby et. al.[12] using the drift tube apparatus. However, we find a substantial effect of source pressure on the observed cross section. As shown in Figure 20, the apparent cross section decreases by a factor of 2 for a factor of 2 increase in source pressure.

As shown in Table VIII we also observe the competitive dissociation process

$$O_3^- \xrightarrow{h\nu} O_2^- + O \qquad \text{(R13)}$$

occurring in the violet and UV portions of the spectrum. Neither product is observed at the shortest wavelength (305 nm) investigated in this work. Since photodestruction of O_3^- in the UV has been observed,[38] our negative result at 305 nm suggests that photodetachment is the predominant process in this region.

G. Positive Ion Dimers

Photodissociation of the dimers Ne_2^+, Ar_2^+, and $(CO_2)_2^+$, has been observed using the dye laser. The dissociation of the CO_2 dimer was also studied using the Hg lamp. Results on the reaction

$$Ar_2^+ \xrightarrow{h\nu} Ar^+ + Ar \qquad \text{(R15)}$$

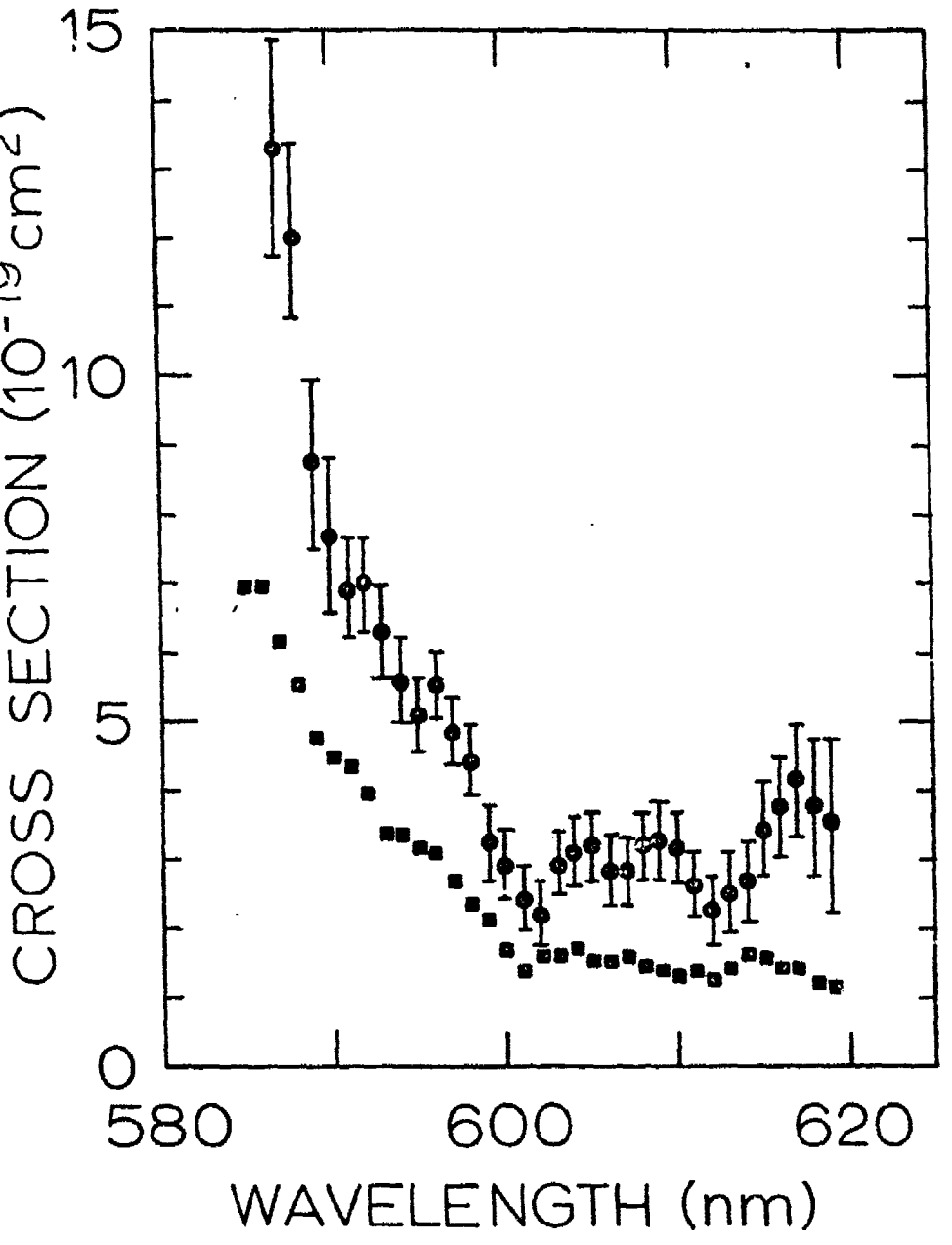

Fig. 20. Photodissociation cross sections for the reaction $O_3^- \rightarrow O^- + O_2$ obtained using the tunable dye laser with Rhodamine 6G, (●) 0.1 torr and (■) 0.2 torr source pressure of pure O_2.

TABLE VIII

Photodissociation Cross Sections For

$O_3^- \rightarrow O^- + O_2$ and $O_3^- \rightarrow O_2^- + O$

λ(nm)	$\sigma(10^{-19}cm^2)$ O^-	O_2^-
305	<1	<1
365	2.2 ± 0.7	1.2 ± 1
405	15 ± 2	15 ± 2
435	59 ± 2	30 ± 2
550	31 ± 1	1.1 ± 0.7
580	12 ± 1	<1
590	4.5 ± 0.5 (1)	<1
600	1.8 ± 0.3 (1)	<1
610	1.3 ± 0.3 (1)	<1

(1) Obtained using tunable dye laser at ion source pressure of 0.1 torr; in this range a significant decrease in cross section with increasing source pressure was observed.

are presented in Figure 21. Over the limited wavelength range studied, there is very little indication of structure as expected for the bound-free transition, $^2\Sigma_u^+ \rightarrow {}^2\Pi_g$, accessible in this energy range. However, as shown in Figure 21, the observed photodisoociation cross section is strongly dependent on ion source pressure. The pressure effect may be rationalized in terms of the potential curves for the $^2\Sigma_u^+$ and $^2\Pi_g$ states calculated by Gilbert and Wahl.[39] The calculated curves are shown in Figure 22, where the $^2\Pi_g$ curve has been displaced downward by 2.0 eV. From these curves it appears that vertical transitions from all vibrational levels of the ground state are possible in the range 2.0 to 2.11 eV studied in this work; however, the transition probability from the ground vibrational state should be quite small at the higher photon energies, but should increase rapidly at wave lengths longer than 620 nm. Therefore, it appears that we are mainly observing transitions from vibrationally excited Ar_2^+ ($^2\Sigma_u^+$) and that the decrease in apparent cross section with increasing source pressure is due to collisional relaxation of the Ar_2^+ ions into the ground vibrational level for which the transition probabilities to the $^2\Pi_g$ state are small for wavelengths shorter than 620 nm.

Results of a single set of measurements on the reaction

$$Ne_2^+ \xrightarrow{h\nu} Ne^+ + Ne \qquad \text{(R14)}$$

are shown in Figure 23. The rather small cross sections observed are rather surprising in view of the potential curves calculated by Gilbert and Wahl,[39] shown in Figure 24. However, more recent ab initio, configuration interaction calculations[40] of the potential curves for Ne_2^+ lead to substantial shifts in these curves and suggest that transitions from the lower vibrational levels of Ne_2^+ ($^2\Sigma_u^+$) to the $^2\Pi_g$ state may not be accessible in this energy range.

The photodissociation technique provides a powerful tool for obtaining

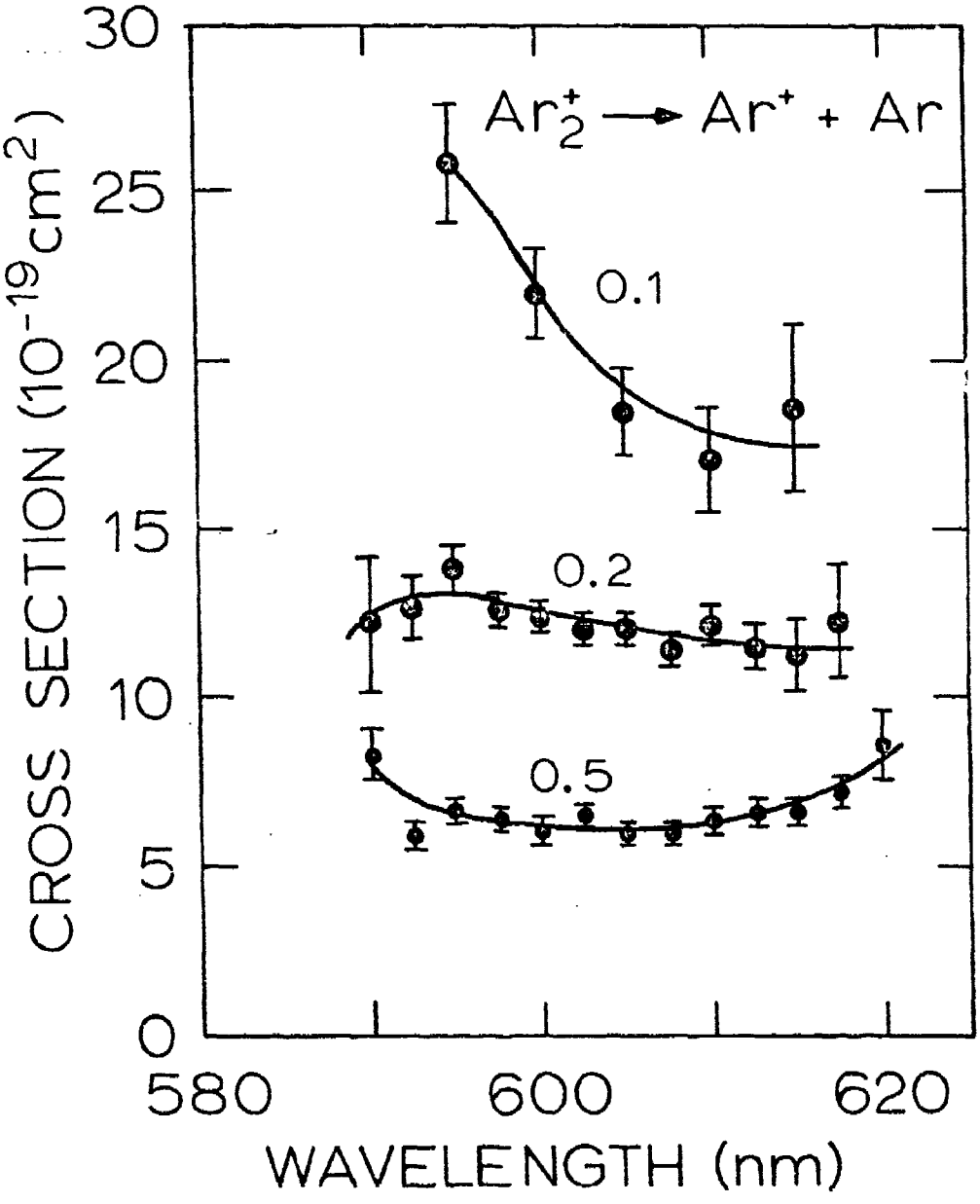

Fig. 21. Cross sections for photodissociation of Ar_2^+ obtained using the tunable dye laser with Rhodamine 6G. The data are labelled with the ion source pressure in torr.

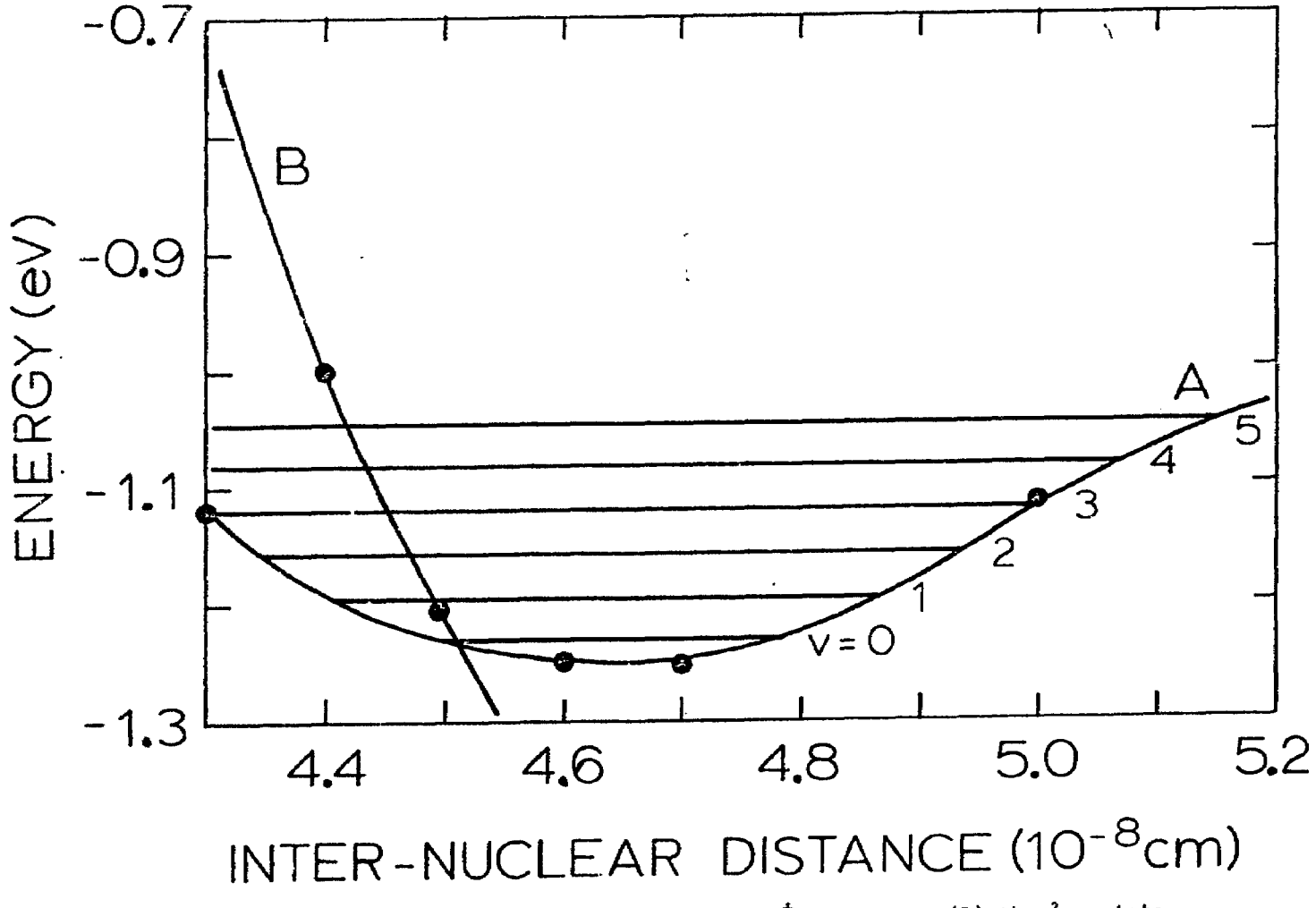

Fig. 22. Potential curves for Ar_2^+ after ref. (39), for (A) the $^2\Sigma_u^+$ state, and (B) the $^2\pi g$ state displaced downward by 20 eV.

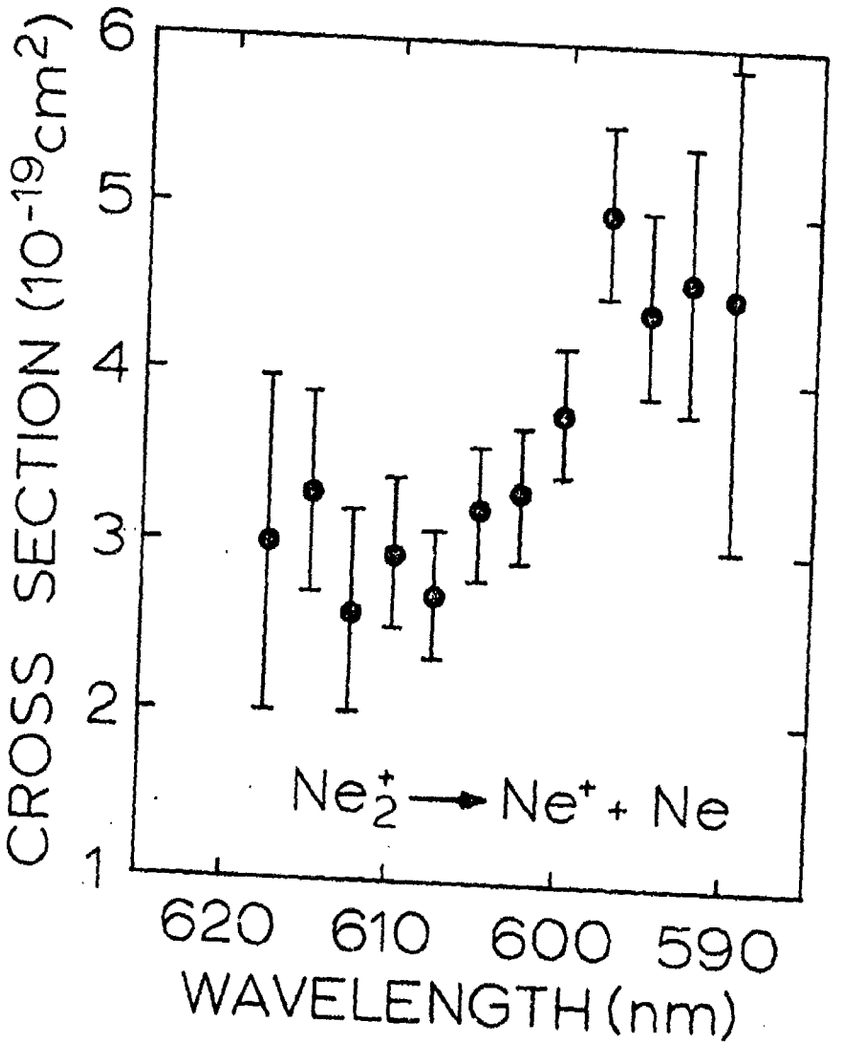

Fig. 23. Cross sections for photodissociation of Ne_2^+ obtained using the tunable dye laser with Rhodamine 6G.

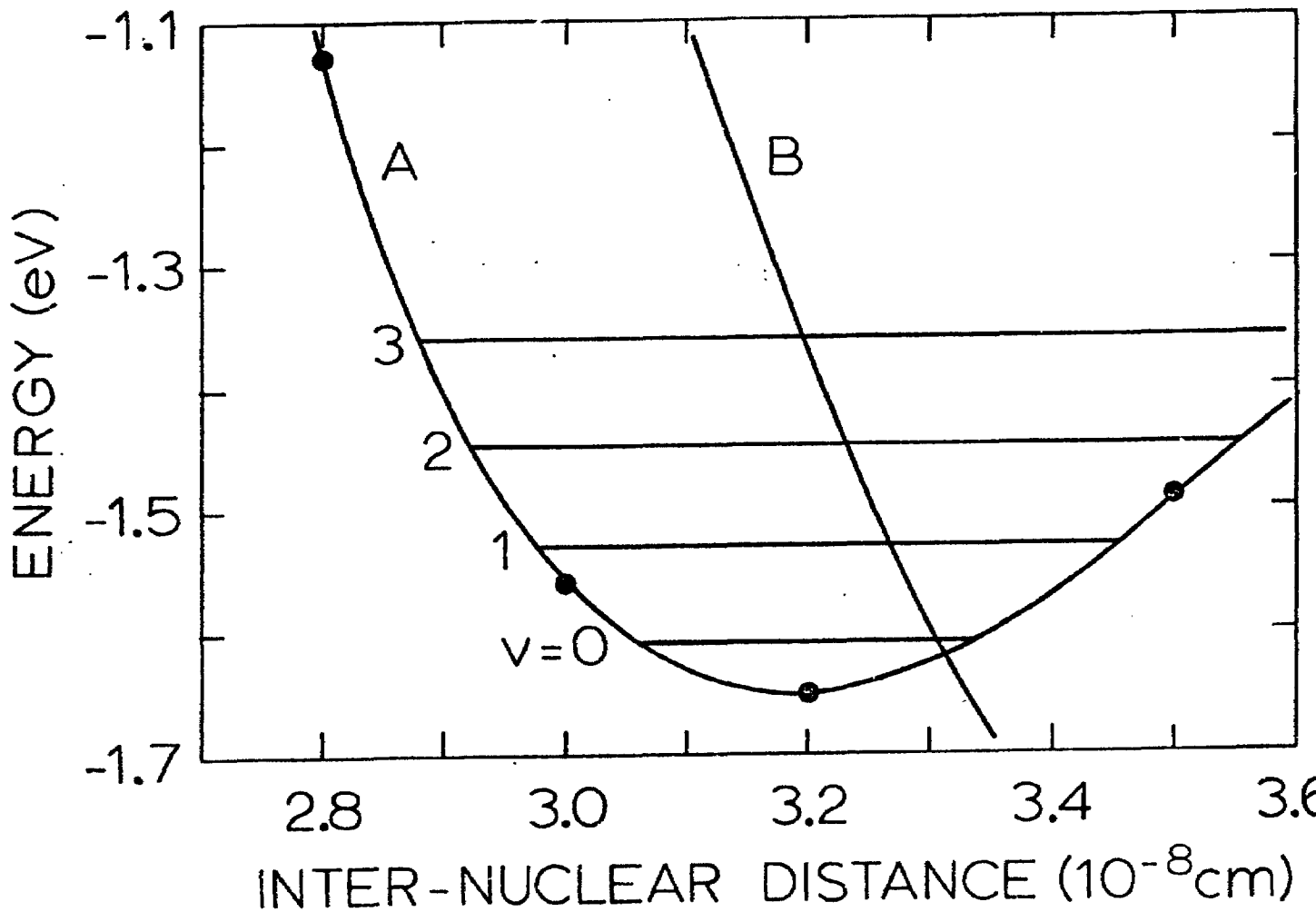

Fig. 24. Potential curves for Ne_2^+ after ref. (39), for (A) the $^2\Sigma_u^+$ state, and (B) the $^2\pi g$ state displaced downward by 2.0 eV.

data on the potential curves for relatively simple systems, such as the rare gas dimer ions. However, to fully exploit the technique we must extend the range of wavelengths employed and measure the kinetic energies of the fragments, in addition to measuring the effect of ion source pressure on the observed photodissociation cross sections.

The reaction

$$(CO_2)_2^+ \xrightarrow{h\nu} CO_2^+ + CO_2 \qquad \text{(R16)}$$

was found to occur in the 600 nm band with the largest cross section of any reaction studied in this work. Results obtained using the dye laser are given in Figure 25. Additional results obtained using the Hg lamp are included in Table IX. The rapid increase observed toward longer wavelengths in the 620 to 627 nm range suggest that the band maximum may lie at even longer wavelengths. In constrast, the observed cross sections in the UV are an order of magnitude smaller. The possibility that dissociation was occurring by other, competing processes at the higher excitation energies was investigated, but no ionic product other than CO_2^+ was observed. Thus it appears that the principle absorption bands for the $(CO_2)_2^+$ ion occur at the red end of the visible spectrum and may extend into the IR. These results suggest that photodissociation of $(CO_2)_2^+$ may be an important reaction in planetary ionospheres such as that of Mars.[2]

V. FUTURE WORK

The results presented in this report demonstrate the utility of photodissociation studies and establish the crossed-beam technique developed in this work as a sensitive and specific method for carrying out these studies. However, some extensions and modifications of the present apparatus would

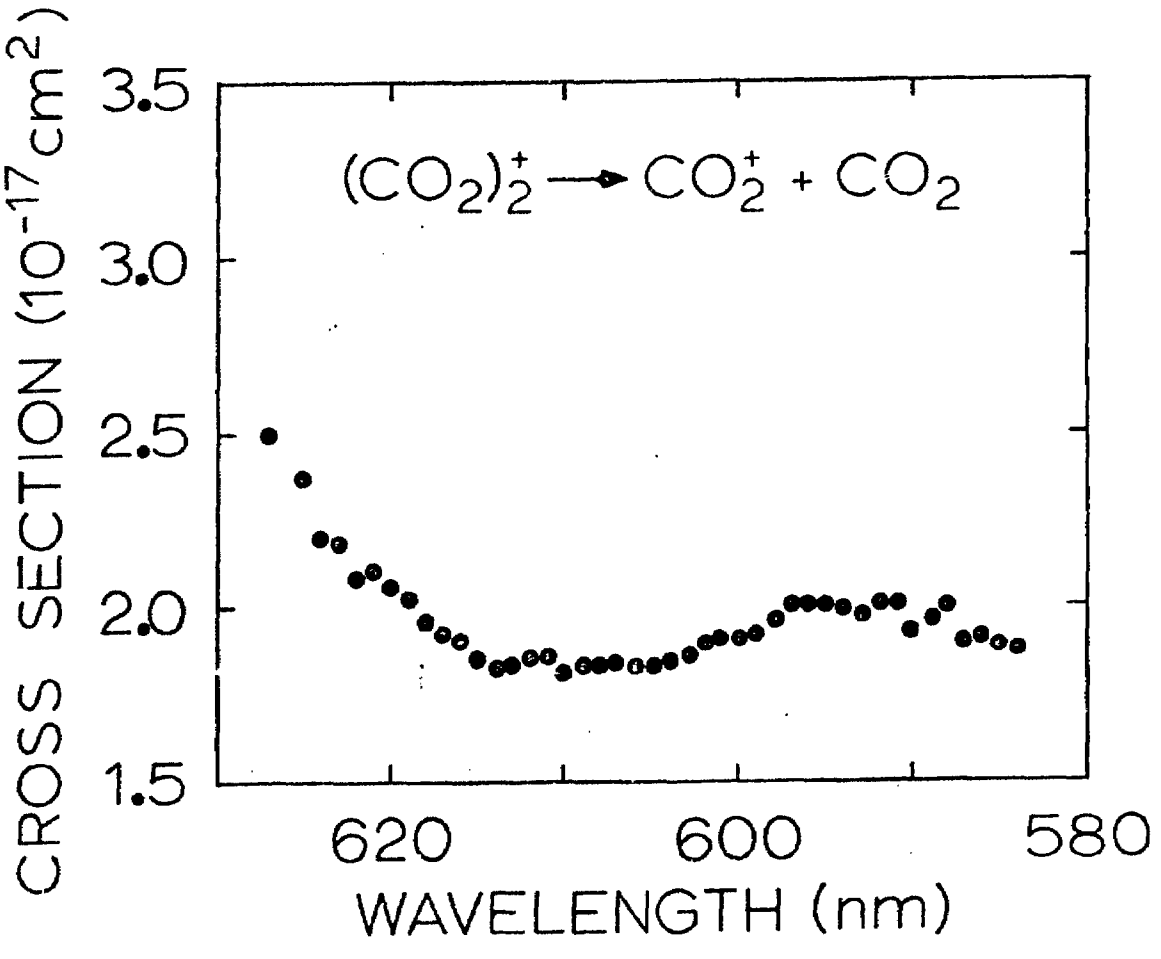

Fig. 25. Cross sections for photodissociation of $(CO_2)_2^+$ obtained using the tunable dye laser with Rhodamine 6G.

TABLE IX

Photodissociation Cross Sections For

$(CO_2)_2^+ \rightarrow CO_2^+ + CO_2$

λ(nm)	σ(10^{-18} cm^2)
305	1.8 ± 0.4
365	1.9 ± 0.3
405	2.0 ± 0.3
435	4.2 ± 0.3
550	16.9 ± 0.2
580	18.9 ± 0.2
590	20.0 ± 0.2
600	19.0 ± 0.2
610	18.3 ± 0.2
620	20.5 ± 0.3
627	25.0 ± 1.0

greatly enhance the overall utility of the results.

A great many more high-resolution measurements of photodissociation cross section as functions of wavelength and ion source conditions are required to fully establish the technique. Interpretation of observed structure requires that the high-resolution measurements span a much wider range of wavelengths than has been accomplished in the present work. Recent advances in tunable dye laser technology make such measurements feasible with the tandem quadrupole instrument developed in the present work. While the present sensitivity is adequate for such studies, the time required for obtaining high-resolution, high-precision results is somewhat excessive. (ca. 24 hours of continuous operation for a typical case) The time required per measurement can be shortened by about an order of magnitude by operating with the ion-photon interaction region within the laser cavity. This modification requires that the laser be fully integrated into the photodissociation apparatus, but it has been shown by Eyler in ICR photodissociation studies that intra-cavity operation is entirely feasible.[41]

A complete study of photodissociation processes requires that all energetically accessible channels be investigated. This has been accomplished in the present work for positive ions, but not for negative ions, since photodetachment is not detected in the present apparatus. A conceptual design change for the photon-ion interaction region has been developed which would allow photoelectrons to be detected as well as negative ions. This design change should be incorporated into the instrument for future work on negative ions.

Finally, a complete description of the photodissociation process requires measurement of the energy and angular distributions of the fragment ions. This measurement definitely requires the use of crossed-beam techniques

with a product mass/energy/angle analyzer such as that used in crossed-beam studies of ion-molecule reactions.[42,43] The photodissociation cross sections measured in present work clearly show that such fundamentally important measurements are now technically feasible.

References

1. E.E. Ferguson in "Interactions Between Ions and Molecules", P. Ausloos, ed., Plenum Press, New York, 1975, p. 313.

2. R. Narcisi, "Interactions Between Ions and Molecules", P. Ausloos, ed., Plenum Press, New York, 1975, p. 635.

3. G.H. Dunn in "Atomic Collision Processes", M.R.C. McDowell, ed., North Holland Publishing Co., Amsterdam, 1964, p. 997.

4. F. von Busch and G.H. Dunn, Phys. Rev. A 5, 1726 (1972).

5. George E. Busch and Kent R. Wilson, J. Chem. Phys., 56, 3626 (1972); 56, 3638 (1972); 56, 3655 (1972).

6. R.W. Diesen, J.C. Wahr, and S.E. Adler, J. Chem. Phys., 55, 2812 (1971).

7. J.B. Ozenne, Pham. D., and J. Durup, Chem. Phys. Lett., 17, 422 (1972).

8. N. van Asselt, J. Maas and J. Loss, private communication cited by J. Durup, 21st Annual Conference on Mass Spectrometry and Allied Topics, San Francisco, California, May 20-25, 1973.

9. R.C. Dunbar, J. Amer. Chem. Soc., 93, 4354 (1971).

10. (a) J.M. Kramer and R.C. Dunbar, J. Amer. Chem. Soc., 94, 4346 (1972).
    (b) R.C. Dunbar, 95, 472 (1973).
    (c) R.C. Dunbar and J.M. Framer, J. Chem. Phys., 58, 1266 (1973).
    (d) R.C. Dunbar and E.W. Fu, J. Amer. Chem. Soc., 95, 2716 (1973).
    (e) R.C. Dunbar, J. Amer. Chem. Soc., 95, 6191 (1973).

11. J.T. Moseley, R.A. Bennett, and J.R. Peterson, Chem. Phys. Lett., 26, 288 (1974); J.T. Moseley, P.C. Cosby, R.A. Bennett, and J.R. Peterson, J. Chem. Phys., 62, 4826 (1975).

12. P.C. Cosby, R.A. Bennett, J.R. Peterson, and J.T. Moseley, J. Chem. Phys., 63, 1612 (1975).

13. NCR Operation, Varian Vacuum Division, 160 Charlemont St., Newton, Mass. 02161, Model VHS-4.

14. Granville-Phillips Co., 5675 E. Arapahoe Ave., Boulder, Colorado 80303, Model 278.

15. Bausch and Lomb, Inc., Rochester, New York 14602. The monochromator is Model 33-86-26-07 and the light source is Model 33=86-36-01.

16. Yellow Springs Instrument Co., Yellow Springs, Ohio.

17. Model CMX-4, Chromatix, 1145 Terra Bella Avenue, Mountain View, California 94043

18. As given by the manufacturer. Results obtained in the present work using Rhodamine 66, were in good agreement with the manufacturer's specification; intersities obtained with Kiton Reds and Cresyl Violet Penchlonate were significantly lower.

19. SSR Insturments Co., 5675 E. Araphoe Ave., Boulder, Colorado 80303.

20. E.E. Ferguson, D.B. Dunkin and F.C. Fehsenfeld, J. Chem. Phys., 57, 1459 (1972).

21. M.L. Vestal and J.H. Futrell, Chem. Phys. Lett., 28, 559 (1974).

22. D.A. Parkes, J.C.S. Faraday Soc. I, 68, 627 (1972).

23. J.L. Morulzi and A.V. Phelps, J. Chem. Phys., 45, 4617 (1966).

24. P.C. Cosby and J.T. Moseley, Phys. Rev. Lett., 34, 1603 (1975).

25. In this work the laser was used with the calibration supplied by the manufacturer. Recent comparison with the HeNe laser line at 623.8 nm showed that the wavelength calibration in this range was giving a reading which was high by approximately 1 ± 0.3 nm.

26. M.E. Jacox and D.A. Milligan, J. Mol. Spectry., 52, 363 (1974).

27. E.E. Ferguson, F.C. Fehsenfeld, and A.V. Phelps, J. Chem. Phys., 59, 1565 (1973).

28. N.G. Adams, D.K. Bohme, D.B. Dunkin, F.C. Fehsenfeld, and E.E. Ferguson, J. Chem. Phys., 52, 3133 (1970).

29. J.A. Burt, J. Chem. Phys., 57, 4649 (1972).

30. C.E. Moore, "Atomic Energy Levels", NBS Circ. 467, Vol. I (1949).

31. G. Henzberg, "Spectra of Diatomic Molecules", Van Nostrand Co., Princeton (1950) p. 560.

32. M. Hallman and I. Lavlicht, J. Chem. Phys., 43, 1508 (1965).

33. D.W. Turner and D.P. May, J. Chem. Phys., 54, 471 (1966).

34. D.C. Frost, S.T. Lee, and C.A. McDowell, Chem. Phys. Lett., 24, 149 (1974).

35. P.J. Hay, T.H. Dunning, Jr., and W.A. Goddard III, J. Chem. Phys., 62, 3912 (1975).

36. D.C. Conway and G.S. Janik, J. Chem. Phys., 53, 1859 (1970).

37. J.L. Pack and A.V. Phelps, J. Chem. Phys., 44, 1870 (1966).

38. J.A. Burt, Ann. Geophys., 28, 607 (1972).

39. T.L. Gilbert and A.C. Wahl, J. Chem. Phys., 47, 3425 (1967).

40. J.S. Cohen and B. Schneider, J. Chem. Phys., 61, 3230 (1974).

41. J.R. Eyler, Rev. Sci. Instr., 45, 1154 (1974).

42. M.L. Vestal, C.R. Blakley, P.W. Ryan and J.H. Futrell, Rev. Sci. Instr., 47, 15 (1976).

43. M.L. Vestal, C.R. Blakley, P.W. Ryan, and J.H. Futrell, J. Chem. Phys., 64, 2094 (1976).

X-RAY LASER EXPERIMENTS

The responsibility assumed by E. M. Eyring and coworkers was the explication of an apparent x-ray laser that had been reported previously by Kepros, Eyring, and Cagle. Repeated failure to detect ~1.5 Å x-rays from the original copper-gel-sandwich targets irradiated with focused Q-switch Nd:glass laser pulses led the group to examine spectrosopically the longer wavelength radiation emitted from laser generated plasmas. The hope was that a population inversion and stimulated emission could be achieved at somewhat longer wavelengths for which the excited state lifetimes would be more nearly comensurate with pumping pulse durations. Herrmann at one time thought he had photographic evidence for stimulated emission at soft x-ray wavelengths, but eventually disproved his own results.

During this same period, Kepros persisted in his own investigations of the "Utah laser" both at Utah and at NASA-Ames. He did not produce results that the rest of the Utah group found convincing, and his employment under the ARL contract was terminated in late summer of 1973.

Another member of the laser group, J. T. Knudtson, used the Nd:glass laser that had been refurbished under the ARL contract to study the stereoisomerism of two thiacarbocyanine dyes irradiated with pulses of frequency doubled (530 nm) laser light. A lengthy manuscript reporting his results and acknowledging ARL assistance has been accepted for publication (subject to minor revision) by the Journal of Physical Chemistry. This work has relevance both for photographic and laser technology since the dyes are used as sensitizers of photographic emulsions and in mode locking of high power lasers.

In early 1974, Herrmann continued to do spectroscopic studies of laser plasmas, but also constructed a laser Raman temperature jump apparatus using the same Nd:glass

laser. This latter device was used in a kinetic study of aqueous methylene blue dimerization that has also been written up for publication with an acknowledgement of ARL assistance.

The present view held by Eyring and coworkers (but not by Kepros or Schalow) is that the "Utah x-ray laser" is not sufficiently reproducible to warrant further study. Even if a convincing explanation for the observed phenomenon does finally emerge, it does not appear likely that it will culminate in a practical x-ray laser. Thus the principal good done by the "Utah laser" was in stimulating a renewed interest in the search for such a device. No further work on the x-ray laser is planned at Utah.